A Non-Linear Model for Elastic Dielectric Crystals With Mobile Vacancies

by J. D. Clayton

NOTICES

Disclaimers

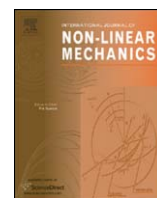# Army Research Laboratory

Aberdeen Proving Ground, MD 21005-5066

A Non-Linear Model for Elastic Dielectric Crystals With Mobile Vacancies

J. D. Clayton
Weapons and Materials Research Directorate, ARL

REPORT DOCUMENTATION PAGE

Form Approved
OMB No. 0704-0188

1. REPORT DATE *(DD-MM-YYYY)*	2. REPORT TYPE	3. DATES COVERED *(From - To)*
July 2009	Reprint	January 2008–January 2009

4. TITLE AND SUBTITLE	5a. CONTRACT NUMBER
A Non-Linear Model for Elastic Dielectric Crystals With Mobile Vacancies	
	5b. GRANT NUMBER
	5c. PROGRAM ELEMENT NUMBER
6. AUTHOR(S)	5d. PROJECT NUMBER
J. D. Clayton	AH80
	5e. TASK NUMBER
	5f. WORK UNIT NUMBER

7. PERFORMING ORGANIZATION NAME(S) AND ADDRESS(ES)	8. PERFORMING ORGANIZATION REPORT NUMBER
U.S. Army Research Laboratory ATTN: RDRL-WMT-D Aberdeen Proving Ground, MD 21005-5066	ARL-RP-253

9. SPONSORING/MONITORING AGENCY NAME(S) AND ADDRESS(ES)	10. SPONSOR/MONITOR'S ACRONYM(S)
	11. SPONSOR/MONITOR'S REPORT NUMBER(S)

12. DISTRIBUTION/AVAILABILITY STATEMENT

Approved for public release; distribution is unlimited.

13. SUPPLEMENTARY NOTES

14. ABSTRACT

A framework is developed for electromechanical behavior of dielectric crystalline solids subjected to finite deformations. The theory is formulated in the context of electrostatics; however, vacancies in the lattice may carry an electric charge, and their concentrations may be large. The material is treated as a continuous body with a continuous distribution of point vacancies, but volumes and charges of individual defects enter the description. The deformation gradient is decomposed multiplicatively into terms accounting for recoverable thermoelasticity and irreversible volume changes associated with vacancies. Thermodynamic arguments lead to constitutive relations among electromechanical quantities framed in the elastically unloaded intermediate configuration, with the Cauchy stress tensor consistently non-symmetric as a result of electrostatic effects. The requirement of non-negative dissipation imposes constraints on vacancy migration. Following postulation of a quadratic form for the free energy potential, a kinetic equation for vacancy flux is derived in the intermediate configuration, with diffusion driven by gradients of vacancy concentration, electrostatic potential, hydrostatic pressure, and crystal structure. Effects of geometric non-linearity (i.e. finite elastic strains and large vacancy concentrations) are found to affect vacancy diffusion in a body subjected to biaxial lattice strain, for example a film device with lattice mismatch at its interfaces.

15. SUBJECT TERMS

electrostatics, non-linear elasticity, diffusion, dielectric, piezoelectric, vacancies, ceramics, defects, electromechanics

16. SECURITY CLASSIFICATION OF:			17. LIMITATION OF ABSTRACT	18. NUMBER OF PAGES	19a. NAME OF RESPONSIBLE PERSON
a. REPORT	b. ABSTRACT	c. THIS PAGE	UU	20	John D. Clayton
Unclassified	Unclassified	Unclassified			19b. TELEPHONE NUMBER *(Include area code)* 410-278-6146

Standard Form 298 (Rev. 8/98)
Prescribed by ANSI Std. Z39.18

A non-linear model for elastic dielectric crystals with mobile vacancies

J.D. Clayton

Impact Physics, U.S. Army Research Laboratory, Aberdeen, MD 21005-5066, USA

A B S T R A C T

A framework is developed for electromechanical behavior of dielectric crystalline solids subjected to finite deformations. The theory is formulated in the context of electrostatics; however, vacancies in the lattice may carry an electric charge, and their concentrations may be large. The material is treated as a continuous body with a continuous distribution of point vacancies, but volumes and charges of individual defects enter the description. The deformation gradient is decomposed multiplicatively into terms accounting for recoverable thermoelasticity and irreversible volume changes associated with vacancies. Thermodynamic arguments lead to constitutive relations among electromechanical quantities framed in the elastically unloaded intermediate configuration, with the Cauchy stress tensor consistently non-symmetric as a result of electrostatic effects. The requirement of non-negative dissipation imposes constraints on vacancy migration. Following postulation of a quadratic form for the free energy potential, a kinetic equation for vacancy flux is derived in the intermediate configuration, with diffusion driven by gradients of vacancy concentration, electrostatic potential, hydrostatic pressure, and crystal structure. Effects of geometric non-linearity (i.e. finite elastic strains and large vacancy concentrations) are found to affect vacancy diffusion in a body subjected to biaxial lattice strain, for example a film device with lattice mismatch at its interfaces.

Published by Elsevier Ltd.

1. Introduction

The present work focuses on electromechanical behavior of dielectric crystalline solids. A dielectric is an insulating material that exhibits polarization in the presence of an electric field. Electromechanical behaviors of interest include piezoelectric, pyroelectric, and ferroelectric effects. Piezoelectricity, in a general sense, refers to the coupling between electric field or polarization and stress or deformation. In continuum theories, piezoelectricity of first order is attributed to the particular choice of free energy functional for the body that may depend, for example, on the product of the strain and the polarization. Such first-order piezoelectric effects can only occur in crystal classes that lack a center of symmetry [43]. Second-order electromechanical effects can arise in non-conductors of all crystal classes as a result of quadratic influences of the electric field. This phenomenon is often called electrostriction [19,20]. Pyroelectric crystals exhibit surface charges when uniformly heated or cooled; such crystals feature energetic coupling between polarization and temperature. The pyroelectric effect is revealed by heating a crystal to induce a change in its polarization. Ferroelectric crystals comprise a subset of pyroelectric crystals, the former exhibiting spontaneous polarity that can be reversed by an applied electric field. Ferroelectric crystals may exhibit a transition temperature, called the Curie point, above which they are not spontaneously polarized; the loss of polarity may accompany a polymorphic phase transition from a non-centrosymmetric to a centrosymmetric structure.

Many theories of geometrically and materially non-linear electromechanics of dielectric solids have appeared in historic and more recent literature. Stratton [57] and Landau and Lifshitz [43] presented formulations encompassing both electrostatics and electrodynamics, though large deformations of the material were not thoroughly considered. Devonshire [20] developed a continuum thermodynamic theory of ferroelectric crystals accounting for material non-linearity, e.g. a higher than quadratic dependence of the free energy upon polarization, but not geometric non-linearity. Toupin [59], Eringen [27], and Tiersten [58] formulated theories of elastic dielectric bodies subjected to arbitrarily large deformations. Tiersten [58] also considered thermal effects and material inertia. Mindlin [52] developed frameworks accounting for spatial gradients of mechanical strain and polarization and demonstrated correlation between higher-order continuum theory and discrete lattice dynamics in the limit of long wavelength behavior. Chowdhury et al. [10] formulated a non-linear theory for thermoelastic dielectrics with effects of polarization gradients. Geometrically non-linear theories of electromechanics were also posited by Maugin [48,49], Hadjigeorgiou

E-mail address: jclayton@arl.army.mil

et al. [30], Dorfmann and Ogden [22], McMeeking et al. [50], and Vu and Steinmann [60]. In some dielectrics, reasonably large strains are feasible via domain switching [64], necessitating the use of geometrically non-linear theory. Large deformations are also attained when pressures are significant enough to suppress fracture, for example in shock physics experiments [49] wherein confined piezoelectric ceramic crystals such as silicon carbide [51] are encountered.

Lattice defects are known to strongly affect electromechanical behavior of dielectric solids and hence performance of engineering devices fabricated from such materials. For example, dislocations accommodate misfit strains between dielectric thin films and substrates in electronic devices [56]. In ionic crystals such as corundum and sodium chloride, consideration of charge distributions and effects of electric fields becomes necessary for describing dislocation motion and dislocation reactions [34,40,41]. Polarized domains and domain walls affect the hysteresis behavior and performance of ferroelectric-based actuator systems [64]. Dislocations [5] and vacancies [8] have been observed in quartz, a piezoelectric crystal used frequently for pressure transducers and resonators. Regarding the latter type of defect, vacancies are observed in a number of dielectric materials and are a focus of the theory developed in the present work. Mobile vacancies, in conjunction with climbing dislocations, can dominate creep deformation, often preferentially to glide-controlled inelasticity at high temperatures [9,61]. In ionic crystals, vacancies typically carry an electric charge [18,37]. Such charged vacancies notably influence dielectric properties and electrical loss characteristics of capacitors, oscillators, and tunable filters [19], for example those comprised of perovskite ceramic crystals such as barium titanate and strontium titanate [16,53]. Electronically active Si and C vacancies are important in silicon carbide [3], a wide band-gap semiconductor.

Some clarification of terminology used for defects is now in order. From an atomistic perspective, a vacancy is regarded as an empty atomic site in the crystal structure, i.e. a missing atom. From the perspective of discrete defects in elastic continua [28], a vacancy can be treated as a sphere on the order of the atomic volume inserted into a slightly larger hole in the solid. The boundary of the hole is then pulled into rigid contact with that of the sphere, resulting in a radial displacement field in the solid that decays with distance from the defect. A void, on the other hand, consists of multiple missing atoms and is typically treated in continuum frameworks as a spherical hole, free of traction along its surface, with dimensions significantly larger than that of a vacancy.

In the present work, a theory for dielectric solids undergoing potentially large volume changes from mobile vacancies is developed, with defects capable of carrying an electric charge. Large deformations resulting from generation and motion voids or vacancies are important when considering large defect concentrations in the vicinity of grain boundary depletion layers [55], and in general when considering coalescence leading to fracture [35]. A finite deformation theory of void nucleation and growth, also incorporating deviatoric dislocation plasticity, was developed by Bammann and Aifantis [2] for ductile metallic crystals, but diffusion and electromechanics were not considered. Finite volumetric deformations arising from point defects, including vacancies and interstitials, were addressed in differential-geometric treatments of Kroner [42] and Clayton et al. [13], but electromechanical effects were not considered. Many and Rakavy [46] considered charge transport resulting from diffusion of various carriers, which may include point defects, but did not consider mechanical deformation. Electrochemical potentials for diffusion of charged atomic species (i.e. self-diffusion or mass transport), interstitials, and vacancies have been the focus of a number of studies [37,40]. The electromechanical behavior of dielectric solids containing mobile vacancies was more recently addressed by Xiao and

co-workers [62,63] and Clayton et al. [14,15]. Related material models have accounted for surface diffusion [14,15,32] and dislocations [14]. Unlike the current work, none accounted for finite volumetric deformations associated with vacancy content.

In the present work, electromechanics of dielectrics in the context of quasi-static electric fields is considered. In the quasi-electrostatic approximation [49,58], finite material velocities are considered, but electrodynamic terms in Maxwell's equations are not. Material velocities are restricted to remain small compared to the speed of light. Free charge densities apart from charges associated explicitly with vacancies, for example free electrons and electron holes, are assumed quasi-static within the dielectric body. This is in contrast to an electrical conductor with free electrons whose motion may lead to substantial current flow, requiring a formal electrodynamic description. The vacancy flux, however, can be interpreted as an effective current whose divergence is proportional to a rate of contribution to the total free charge density from vacancies, in which case the dielectric with charged defects can be formally classified as a semiconductor. Neither magnetic effects nor mass transport (i.e., self-diffusion of bulk atoms or interstitials) is considered here.

The remainder of this paper is organized as follows. First, governing relationships for geometrically non-linear electrostatics—Maxwell's equations, momentum and energy balances, and the dissipation inequality in the context of finite deformations—are reviewed. Such a review is necessary to accompany derivations that follow. A geometrically non-linear theory for elastic dielectrics, first in the absence of defects, is presented. Constitutive relations for elastic dielectric solids emerge, following consideration of the dissipation inequality [10,17,24,30,50]. Then, following similar mathematical and physical arguments, a geometrically non-linear theory of dielectric crystals containing mobile vacancies is developed. The vacancies may support an electric charge as often occurs in ionic solids or may be electrically neutral as a special case more applicable, for example, in monatomic crystals. The theory presented here extends previous work [14,15] to large deformations and to situations wherein Maxwell's stress is non-negligible, though surface diffusion and surface growth considered previously are not considered here. Rather, particular attention is directed towards the diffusion equation for the bulk vacancy flux. Lastly, effects of large elastic deformations and large vacancy concentrations on diffusion of vacancies are examined for a slab subjected to biaxial lattice strain, for example a film with residual stresses due to lattice mismatch [14,53].

The following notation is used. Vector and tensor quantities are written in bold type, while scalars and individual components are written in italics. The index notation follows the Einstein summation convention, distinguishing between covariant (subscript) and contravariant (superscript) components. Current configuration indices are written in lower case Latin, reference configuration indices in upper case Latin, and intermediate configuration indices are denoted by Greek symbols. Juxtaposition implies summation over two repeated adjacent indices (e.g. $(\mathbf{AB})_a^{.b} = A_{ac}B^{cb}$). The dot product of vectors is represented by the symbol • (e.g. $\mathbf{a} \cdot \mathbf{b} = a^a g_{ab} b^b$, with g_{ab} components of a metric). Angled brackets denote a dual (scalar) product (e.g. $\langle \mathbf{A}, \mathbf{B} \rangle = tr(\mathbf{AB}) = A_{ab}B^{ba}$ and $\langle \boldsymbol{\alpha}, \mathbf{b} \rangle = \alpha_a b^a$). The colon denotes contraction over repeated pairs of indices (e.g. $\mathbf{A} : \mathbf{B} = tr(\mathbf{A}^T\mathbf{B}) = A_{ab}B^{ab}$ and $(\mathbf{C} : \mathbf{A})^{ab} = C^{abcd}A_{cd}$). The symbol $\otimes$ represents the tensor product (e.g., $(\mathbf{a} \otimes \mathbf{b})^{ab} = a^a b^b$). The symbol $\circ$ represents the composition, such that for two functions f and g, $(f \circ g)(X) = f(g(X))$. Superposed -1, T, and • denote inverse, transpose, and material time derivative operations, respectively. Subscripted commas denote partial coordinate differentiation. Indices in parentheses are symmetric, that is $2A^{(ab)} = A^{ab} + A^{ba}$, while indices in brackets are anti-symmetric, i.e., $2A^{[ab]} = A^{ab} - A^{ba}$. An extensive list of symbols is provided in Appendix A.

2. Geometrically non-linear electromechanics

Field variables associated with finite deformations and electromechanical effects are introduced in Section 2.1, followed by governing equations of electrostatics in Section 2.2. In Sections 2.3, 2.4 and 2.5, equations of momentum and energy conservation and the dissipation inequality for dielectric solids subjected to finite deformations and electromechanical loadings are presented.

2.1. Kinematics and electromechanical quantities

Let $\mathbf{x} = \varphi(\mathbf{X}, t)$ denote the smooth and invertible motion of a body, with $\mathbf{x}$ denoting spatial coordinates and $\mathbf{X}$ denoting reference coordinates. The deformed body B is parameterized by spatial coordinates, while the body B_0 in the reference configuration is parameterized by reference coordinates. The local deformation gradient is the map from the reference to current tangent space, $T_X B_0 \rightarrow T_x B$ [47]

$$\mathbf{F} = T\varphi_X = \frac{\partial x^a}{\partial X^A} \mathbf{g}_a \otimes \mathbf{G}^A, \quad F^a_{.A} = \frac{\partial x^a}{\partial X^A}, \tag{1}$$

where $\mathbf{g}_a$ and $\mathbf{G}^A$ are bases referred to current and reference coordinates, respectively. A differential line element $d\mathbf{X} \in T_X B_0$ is deformed to $d\mathbf{x} = \mathbf{F}\, d\mathbf{X} \in T_x B$. Mass conservation provides the requirements

$$\int_V \rho_0 \, dV = \int_v \rho \, dv \rightarrow \rho_0 = \rho J, \tag{2}$$

where reference and current mass densities are ρ_0 and ρ, reference and current volume elements are dV and dv, and the Jacobian $J = dv/dV = \det(F^a_{.A})\sqrt{g/G} > 0$, with $g = \det(g_{ab})$ and $G = \det(G_{AB})$. Spatial and referential metric tensors satisfy $g_{ab} = \mathbf{g}_a \cdot \mathbf{g}_b$ and $G_{AB} = \mathbf{G}_A \cdot \mathbf{G}_B$. Christoffel symbols are

$$2\overset{g}{\Gamma}{}^{..a}_{bc} = g^{ad}(g_{cd,b} + g_{bd,c} - g_{bc,d}),$$
$$2\overset{G}{\Gamma}{}^{.A}_{BC} = G^{AD}(G_{CD,B} + G_{BD,C} - G_{BC,D}). \tag{3}$$

Components of the covariant derivative of a spatial vector field $\mathbf{a} \in TB$ are then $\overset{g}{\nabla}_b a^a = a^a_{,b} + \overset{g}{\Gamma}{}^{..a}_{bc} a^c$. Analogous formulae apply for the covariant derivative $\overset{G}{\nabla}_B$ taken with respect to reference coordinates, and covariant derivatives of higher-rank tensors follow conventional definitions [13]. Specifically let $\mathbf{v}(\mathbf{x}, t)$ denote the spatial velocity field. The spatial velocity gradient is

$$L^a_{.b} = \overset{g}{\nabla}_b v^a = v^a_{,b} + \overset{g}{\Gamma}{}^{..a}_{bc} v^c = \dot{F}^a_{.A} F^{-1A}_{.b}. \tag{4}$$

Furthermore, let $E_{AB} = (\tfrac{1}{2})(C_{AB} - G_{AB})$ denote components of the symmetric Lagrangian strain tensor, where $C_{AB} = F^a_{.A} g_{ab} F^b_{.B}$. It follows that $\dot{J} = J D^a_{.a}$ and $\dot{E}_{AB} = F^a_{.A} D_{ab} F^b_{.B}$, where $D_{ab} = L_{(ab)}$.

The spatial electric field $\hat{\mathbf{e}} \in TB$ describes the Lorentz force $\hat{\mathbf{f}}$ associated with a point charge of magnitude q: $\hat{\mathbf{f}} = q\hat{\mathbf{e}}$. The electric field may permeate the dielectric body, surrounding media, and vacuum. The electric field vanishes inside conductors in the absence of current flow.

The free charge density per unit spatial volume is defined by

$$\hat{\rho} = \sum_i \hat{n}^{(i)} q^{(i)} = \sum_i \hat{n}^{(i)} e z^{(i)}, \tag{5}$$

with $\hat{n}^{(i)}$ the number of charge carriers per unit volume of charge $q^{(i)} = e z^{(i)}$, where e is the charge of an electron ($1.602(10)^{-19}$ C) and $z^{(i)}$ is the integer valence of each member of charge carrier population i. For excess electrons, $z = -1$, while for holes or missing electrons, $z = +1$. The charge density $\hat{\rho}$ vanishes in pure vacuum (i.e., a vacuum containing no free electrons) and within neutral conductors.
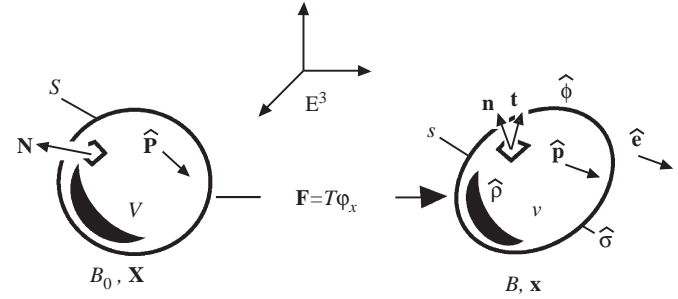

Fig. 1. Continuum quantities for deforming dielectric body in presence of electric field.

Polarization density, or simply the polarization, is the vector $\hat{\mathbf{p}} \in T_x B$ (dimensions of charge per unit area) that is often collinear with the relative shift of electron clouds and/or ions comprising a dielectric, or with the orientation of a permanent electric dipole [49]. Polarization vanishes in vacuum and in conductors. Electric displacement $\hat{\mathbf{d}} \in TB$ is related to electric field and polarization by [57]

$$\hat{\mathbf{d}} = \varepsilon_0 \hat{\mathbf{e}} + \hat{\mathbf{p}}, \tag{6}$$

where the dimensional constant $\varepsilon_0(8.854(10)^{-12}\,\text{C}^2\,\text{N}^{-1}\,\text{m}^{-2})$ is the permittivity of free space. Since polarization vanishes in vacuum, (6) reduces to $\hat{\mathbf{d}} = \varepsilon_0 \hat{\mathbf{e}}$ in free space. The surface free charge density $\hat{\sigma}$ is defined on surface s of a body with unit normal $\mathbf{n}$ as

$$\hat{\sigma} = \langle [\![\hat{\mathbf{d}}]\!], \mathbf{n} \rangle. \tag{7}$$

In (7), $[\![\hat{\mathbf{d}}]\!] = \hat{\mathbf{d}}^+ - \hat{\mathbf{d}}^-$ is the jump in $\hat{\mathbf{d}}$ at the interface of s and the medium external to the body, which could be vacuum or another body. Here, + and − denote respective limiting values of a quantity at locations outside and inside the body as s is approached from the corresponding side, and $\mathbf{n}$ is directed from the − side to the + side (directed from inside to outside). A deforming dielectric body in three-dimensional Euclidean space E^3 with corresponding electromechanical quantities is shown in Fig. 1.

2.2. Maxwell's equations of electrostatics

Maxwell's equations of electrostatics consist of the following integral relations in the spatial frame:

$$\int_c \hat{\mathbf{e}} \cdot d\mathbf{x} = 0, \quad \int_s \langle \hat{\mathbf{d}}^-, \mathbf{n} \rangle \, ds = \int_v \hat{\rho} \, dv. \tag{8}$$

The first of Maxwell's equations states that the line integral of the electric field along an arbitrary closed curve c vanishes. From Stokes's theorem, the first of (8) can be written

$$\int_c \hat{e}_a \, dx^a = \int_s \varepsilon^{abc} \overset{g}{\nabla}_a \hat{e}_b n_c \, ds = 0. \tag{9}$$

A vector field in a simply connected domain whose skew covariant derivative (i.e. curl) vanishes can be represented as the gradient of a scalar potential. Here, the scalar potential $\hat{\phi}$ is called the electrostatic potential and is continuous throughout space [27]. The local form of (9) is[1]

$$\varepsilon^{abc} \overset{g}{\nabla}_a \hat{e}_b = 0 \Leftrightarrow \hat{e}_{[b,a]} = -\hat{\phi}_{[,ba]} = 0 \Leftrightarrow \hat{e}_b = -\hat{\phi}_{,b}. \tag{10}$$

---

[1] Though curvilinear coordinates are used throughout the paper for generality, Cartesian indices are implied for all integral equations involving vector and tensor fields. Alternatively, following [59], all quantities entering a vector-valued integrand can be parallel transported to a single point using the shifter, and the resultant integral evaluated at that point.

In the domain of (9), C^1-continuity of $\hat{\mathbf{e}}$ is assumed; finite jumps in the normal component of $\hat{\mathbf{e}}$ are admitted across surfaces of discontinuity, but $\varepsilon^{abc}[\![\hat{e}_b]\!]n_c = 0$ across such surfaces [27]. The second of Maxwell's equations establishes a conservation law between surface and volumetric charges. Applying the divergence theorem to the left side of the second of (8) and localizing the result

$$\overset{g}{\nabla}_a \hat{d}^a = \hat{\rho}. \tag{11}$$

In arriving at (11), C^1-continuity of $\hat{\mathbf{d}}$ is assumed within the domain of integration; the normal component of a jump in $\hat{\mathbf{d}}$ across a surface is given by (7). Multiplying (11) by $\hat{\phi}$, integrating over volume v enclosed by surface s, and applying the divergence theorem with (7) and (10) yields

$$\int_v \hat{\mathbf{d}} \cdot \hat{\mathbf{e}}\, dv = \int_v \hat{\rho}\hat{\phi}\, dv + \int_s \hat{\omega}\hat{\phi}\, ds, \tag{12}$$

where $\hat{\omega} = -\langle \hat{\mathbf{d}}^-, \mathbf{n} \rangle$ measures the contribution from the inside of s to the free charge density in (7).

Spatial relations (8)–(12) can be mapped to their referential counterparts as follows [22,60]. In particular, the first of (8) becomes

$$\int_c \hat{\mathbf{e}} \cdot d\mathbf{x} = \int_C \hat{\mathbf{e}} \cdot \mathbf{F}\, d\mathbf{X} = \int_C \mathbf{F}^T \hat{\mathbf{e}} \cdot d\mathbf{X} = \int_C \hat{\mathbf{E}} \cdot d\mathbf{X} = 0, \tag{13}$$

where C is a closed reference curve and $\hat{\mathbf{E}} = \mathbf{F}^T \hat{\mathbf{e}} \in TB_0$, with $\hat{E}_A = F_A^a \hat{e}_a$. Relations analogous to (10) then emerge

$$\varepsilon^{ABC} \overset{G}{\nabla}_A \hat{E}_B = 0 \Leftrightarrow \hat{E}_{[B,A]} = -\hat{\Phi}_{[,BA]} = 0 \Leftrightarrow \hat{E}_B = -\hat{\Phi}_{,B}, \tag{14}$$

where the potential $\hat{\Phi}(\mathbf{X}, t) = \hat{\phi} \circ \varphi$. From Nanson's formula

$$\int_S \langle \hat{\mathbf{D}}^-, \mathbf{N} \rangle\, dS = \int_V \hat{\rho}_0\, dV, \tag{15}$$

with $\hat{\mathbf{D}} = J\mathbf{F}^{-1}\hat{\mathbf{d}} \in TB_0$, $\hat{\rho}_0 = \hat{\rho}J$, and S the surface enclosing reference volume V. The analog of (11) is then obtained directly from (15) and the divergence theorem

$$\overset{G}{\nabla}_A \hat{D}^A = \hat{\rho}_0. \tag{16}$$

Finally, multiplying both sides of (16) by $\hat{\Phi}$, integrating over V, and using (14) gives

$$\int_V \hat{\mathbf{D}} \cdot \hat{\mathbf{E}}\, dV = \int_V \hat{\rho}_0 \hat{\Phi}\, dV - \int_S \hat{\Phi}\langle \hat{\mathbf{D}}^-, \mathbf{N} \rangle\, dS. \tag{17}$$

No natural definition exists for the reference analog of spatial polarization $\hat{\mathbf{p}}$. One obvious assumption is

$$\hat{\mathbf{P}} = \mathbf{F}^T \hat{\mathbf{p}}, \tag{18}$$

leaving the following referential version of (6):

$$\hat{\mathbf{D}} = J\mathbf{C}^{-1}(\varepsilon_0 \hat{\mathbf{E}} + \hat{\mathbf{P}}), \tag{19}$$

where the symmetric deformation tensor $\mathbf{C}$ is defined immediately following (4).

Some authors partition the electric field or electrostatic potential into contributions from various internal and external sources [27,59]; in the present work, a single electric field and potential are used in the governing equations, following [58].

2.3. Momentum conservation

Electromechanical interactions induce modifications to the balance laws of linear and angular momentum of classical continuum mechanics. Such interactions can be addressed straightforwardly via the introduction of an electromechanical body force. In electrostatics, this force, per unit current volume, is

$$\hat{\mathbf{b}} = \hat{\mathbf{p}}\overset{\mathbf{g}}{\nabla}\hat{\mathbf{e}} + \hat{\rho}\hat{\mathbf{e}}, \quad \hat{b}^a = \hat{p}^b \overset{g}{\nabla}_b \hat{e}^a + \hat{\rho}\hat{e}^a, \tag{20}$$

where the first term on the right side is attributed to short range interaction of the polarization with the electric field [58,59], and the second term arises from Lorentz forces attributed to non-vanishing free charges. From (6), (10) and (11), and assuming sufficient smoothness of the electric field and polarization, the force $\hat{\mathbf{b}}$ can be expressed as the divergence of a rank two contravariant tensor known as the Maxwell stress $\hat{\boldsymbol{\tau}}$

$$\hat{\boldsymbol{\tau}} = \hat{\mathbf{e}} \otimes \hat{\mathbf{d}} - \frac{\varepsilon_0}{2}(\hat{\mathbf{e}} \cdot \hat{\mathbf{e}})\mathbf{g}^{-1}$$
$$= \hat{\mathbf{e}} \otimes \hat{\mathbf{p}} + \varepsilon_0 \hat{\mathbf{e}} \otimes \hat{\mathbf{e}} - \frac{\varepsilon_0}{2}(\hat{\mathbf{e}} \cdot \hat{\mathbf{e}})\mathbf{g}^{-1}, \quad \overset{g}{\nabla}_b \hat{\tau}^{ab} = \hat{b}^a. \tag{21}$$

With the inclusion of electrostatic body force $\hat{\mathbf{b}}$, the global balance of linear momentum is

$$\int_v \rho \dot{v}^a\, dv = \int_s t^a\, ds + \int_v (\bar{b}^a + \hat{b}^a)\, dv = \int_v (\overset{g}{\nabla}_b \sigma^{ab} + \bar{b}^a + \hat{b}^a)\, dv, \tag{22}$$

with $t^a = \sigma^{ab}n_b$ the mechanical traction, $\boldsymbol{\sigma}$ the Cauchy stress, and $\bar{\mathbf{b}}$ the mechanical body force per unit current volume. In (22), the Cauchy stress is assumed differentiable within v. The local form of (22) is

$$\overset{g}{\nabla}_b \tau^{ab} + \bar{b}^a = \rho \dot{v}^a, \tag{23}$$

where $\boldsymbol{\tau} = \boldsymbol{\sigma} + \hat{\boldsymbol{\tau}}$ is the total stress tensor, i.e., the sum of the Cauchy and Maxwell stresses. Because the electric field and polarization may exhibit jump discontinuities across s, the boundary conditions are

$$T^a = t^{-a} - [\![\hat{\tau}^{ab}]\!]n_b, \tag{24}$$

where T^a are components of the net applied traction [59], which can be assigned as $T^a = t^{+a}$ [58].

The body force $\hat{\mathbf{b}}$ likewise enters the balance of moment of momentum, along with an additional moment attributed to interaction between the polarization and electric field [58,59]

$$\frac{d}{dt} \int_v \varepsilon_{abc}x^b \rho v^c\, dv = \int_v \varepsilon_{abc}x^b \bar{b}^c\, dv + \int_s \varepsilon_{abc}x^b t^c\, ds$$
$$+ \int_v \varepsilon_{abc}x^b \hat{b}^c\, dv + \int_v \varepsilon_{abc}\hat{e}^c \hat{p}^b\, dv. \tag{25}$$

Application of the divergence theorem and Reynolds transport theorem along with (21) leads to

$$\int_v \varepsilon_{abc}x^b(\rho \dot{v}^c - \bar{b}^c - \overset{g}{\nabla}_d \tau^{cd})\, dv = \int_v \varepsilon_{abc}(\sigma^{cb} + \rho v^c v^b + \hat{\tau}^{cb})\, dv. \tag{26}$$

The left side of (26) vanishes by linear momentum balance (23), and the second term in the integrand on the right vanishes by the symmetry of $\mathbf{v} \otimes \mathbf{v}$. The local balance of angular momentum is, from the remaining terms in (26),

$$\tau^{ab} = \tau^{(ab)}, \quad \sigma^{[ab]} = \hat{\tau}^{[ba]} = \hat{e}^{[b}\hat{p}^{a]}, \tag{27}$$

meaning that the total stress $\boldsymbol{\tau}$ is symmetric, but the Cauchy stress $\boldsymbol{\sigma}$ need not be. In non-polarized media, $\hat{e}^{[a}\hat{p}^{b]} = 0$ such that the classical balance of angular momentum $\sigma^{[ab]} = 0$ applies. However, if such materials support an electric field and a non-vanishing free charge density, the balance of linear momentum (23) will be affected by (20). In pure vacuum, the Cauchy stress vanishes, and the balance of linear momentum reduces to $\overset{g}{\nabla}_b \hat{\tau}^{ab} = \hat{b}^a = 0$, satisfied identically since the polarization and free charge density vanish by definition in pure vacuum.

Various definitions have been postulated for the mechanical stress and Maxwell stress, as discussed by Eringen [27]. The definition used in the present work for the Cauchy stress corresponds to the local stress of Toupin [59] and is the transpose of the mechanical stress of Tiersten [58]. The definition used in the present work for the Maxwell stress (21) is consistent with that of Toupin [59] and is the transpose of the Maxwell stress of Tiersten [58]. Notice that in the present work, the index of the traction vector corresponds to the first index of the corresponding stress tensor (e.g. $t^a = \sigma^{ab} n_b$), following the notation scheme of Toupin [59], but opposite to notations of Eringen [27], Tiersten [58], and McMeeking et al. [50].

2.4. Energy conservation

Various methods have been set forth to account for energy conservation in dielectrics [10,14,15,20,27,48–50,58–60]. Variational principles can provide insight into field equations and boundary conditions for static and non-dissipative processes [27,59], while rate forms of the energy balance are useful for situations involving dynamics and dissipation [14,15,50,58]. Prescribed here is a global balance between rates of internal energy, kinetic energy, external work, and thermochemical heating

$$\frac{d}{dt}(\mathscr{E} + \mathscr{K}) = \mathscr{P} + \mathscr{Q}, \tag{28}$$

with the contributions from kinetic energy $\mathscr{K}$ and extrinsic thermochemical energy $\mathscr{Q}$ given by

$$\mathscr{K} = \int_v (\rho/2)\mathbf{v}\boldsymbol{\cdot}\mathbf{v}\,dv, \quad \mathscr{Q} = \int_v \rho r\,dv - \int_s \langle\mathbf{q}^-, \mathbf{n}\rangle\,ds, \tag{29}$$

where a dielectric body occupying spatial volume v with oriented surface element $\mathbf{n}\,ds$ is considered. Field variables are assumed to possess sufficient smoothness within v to enable use of local forms of Maxwell's equations and momentum balances as well as the divergence theorem. However, electric field and polarization may exhibit finite jumps across s. In the present thermodynamic analysis, the body is treated as an open region, meaning that surface terms are evaluated as s is approached from the inside of the body. In the second of (29), scalar r denotes sources of thermal or chemical energy per unit mass, and $\mathbf{q} \in T_xB$ is the heat flux vector that is continuous across all interfaces such that $\langle[\![\mathbf{q}]\!], \mathbf{n}\rangle = 0$ along s [58]. The total internal energy is defined by

$$\mathscr{E} = \int_v \rho e\,dv + \frac{\varepsilon_0}{2}\int_v \hat{\mathbf{e}}\boldsymbol{\cdot}\hat{\mathbf{e}}\,dv. \tag{30}$$

The first term on the right accounts for the stored internal energy of the body, denoted locally per unit mass by e. The second term on the right side of (30) represents the potential energy of the electric field that permeates the body and underlying vacuum (i.e. the aether). The combined electromechanical rate of working is

$$\mathscr{P} = \int_s \mathbf{t}\boldsymbol{\cdot}\mathbf{v}\,ds + \int_v (\bar{\mathbf{b}} + \hat{\mathbf{b}})\boldsymbol{\cdot}\mathbf{v}\,dv + \frac{d}{dt}\int_s \hat{\omega}\hat{\phi}\,ds$$
$$+ \frac{d}{dt}\int_v \hat{\rho}\hat{\phi}\,dv + \int_v \Omega\,dv. \tag{31}$$

The first term on the right of (31) accounts for the mechanical traction, the second term accounts for body forces, the third term accounts for the work done by surface charges, and the fourth for the work of volumetric charges. The final term is chosen such that throughout E^3 (moving dielectric and vacuum) the balance of energy is satisfied identically:

$$\Omega = [\dot{\hat{\phi}}_{,a} - \hat{\phi}_{,b}\overset{g}{\nabla}_a v^b + \hat{\phi}_{,a}\overset{g}{\nabla}_b v^b]\hat{d}^a + \frac{\varepsilon_0}{2}\hat{\phi}_{,a}\hat{\phi}^{,a}\overset{g}{\nabla}_b v^b, \tag{32}$$

where application of the chain rule produces the identity $\dot{\hat{\phi}}_{,a} = \hat{\phi}_{,b}\overset{g}{\nabla}_a v^b - \dot{\hat{e}}^a$. Various forms have been suggested for Ω [27,49,58], and some authors subtract part or all of the contribution of Ω from the rate of total internal energy rather than incorporate it in the rate of external power. Identical quantities can be represented in a vast number of ways via manipulation of Maxwell's equations and use of vector identities and theorems of Gauss and Stokes. Recall also that in the present Section, along the lines of previous theories for dielectric media in the quasi-electrostatic approximation [10,50,58], purely mechanical dynamic effects are considered (i.e. finite velocity $\mathbf{v}$), but electrodynamics are not (i.e., fluxes of free electrons/holes are absent).

Substituting (29)–(32) into (28) and converting all surface integrals to volume integrals using (12) and the divergence theorem, the global balance of energy becomes

$$\left[\int_v \rho\dot{e}\,dv + \int_v \rho\dot{v}^a v_a\,dv - \int_v \hat{e}_a\dot{\hat{p}}^a\,dv\right] + \int_v \hat{e}_a\dot{\hat{d}}^a\,dv + \frac{\varepsilon_0}{2}\int_v \hat{e}_a\hat{e}^a\overset{g}{\nabla}_b v^b\,dv$$
$$= \left[\int_v \rho r\,dv - \int_v \overset{g}{\nabla}_b q^b\,dv + \int_s (\overset{g}{\nabla}_b\sigma^{ab} v_a + \sigma^{ab}\overset{g}{\nabla}_b v_a)\,dv\right.$$
$$\left. + \int_v (\bar{b}^a + \hat{b}^a)v_a\,dv\right] + \int_v \hat{e}_a\dot{\hat{d}}^a\,dv + \frac{\varepsilon_0}{2}\int_v \hat{\phi}_{,a}\hat{\phi}^{,a}\overset{g}{\nabla}_b v^b\,dv$$
$$+ \int_v (\dot{\hat{e}}_a + \dot{\hat{\phi}}_{,a} - \hat{\phi}_{,b}\overset{g}{\nabla}_a v^b + \hat{\phi}_{,a}\overset{g}{\nabla}_b v^b + \hat{e}_a\overset{g}{\nabla}_b v^b)\hat{d}^a\,dv. \tag{33}$$

The integrand of the last term on the right side of (33) vanishes identically. Terms in braces vanish identically in vacuum, and terms not in braces cancel. Collecting terms in braces and localizing gives

$$\rho\dot{e} = (\overset{g}{\nabla}_b\tau^{ab} + \bar{b}^a - \rho\dot{v}^a)v_a + \sigma^{ab}\overset{g}{\nabla}_b v_a - \overset{g}{\nabla}_b q^b + \rho r + \hat{e}_a\dot{\hat{p}}^a. \tag{34}$$

Then after using (4) and (23), the local balance of energy remains

$$\rho\dot{e} = \langle\boldsymbol{\sigma}, \mathbf{L}^T\rangle - \langle\overset{\mathbf{g}}{\nabla}, \mathbf{q}\rangle + \rho r + \langle\hat{\mathbf{e}}, \dot{\hat{\mathbf{p}}}\rangle. \tag{35}$$

Notice that (35) differs from the energy balance for non-polar continua in two ways. Firstly, the Cauchy stress is not necessarily symmetric in (35), so that the spin (skew part) of $\mathbf{L}$ may contribute to the stress power $\langle\boldsymbol{\sigma}, \mathbf{L}^T\rangle = \sigma^{ab}L_{ab} = \sigma^{ab}\overset{g}{\nabla}_b v_a$. Since $t^a = \sigma^{ab}n_b$, the index of stress associated with the traction vector is conjugate to that associated with the velocity v^a, in agreement with other non-linear theories for dielectric media [58] and also in agreement with models of generalized continua with couple stresses [45]. Secondly, the final term on the right side of (35) is absent in non-polar solids.

Two approximations are often made to simplify the governing equations of deformable dielectrics. The first is the assumption of geometric linearity, i.e. small deformations. In that case introduction of (13)–(19) is unnecessary, since the distinction between undeformed and deformed configurations is not made explicitly. Balances (23) and (27) are unchanged, but (35) becomes $\rho\dot{e} = \sigma^{ab}\nabla_b\dot{u}_a - \nabla_b q^b + \rho r + \hat{e}_a\dot{\hat{p}}^a$, where $\mathbf{u}$ is the displacement. The second is the assumption that terms on the order of the product of the electric field and polarization, or on the order of the square of the electric field, may be neglected in the governing equations [54]. In that case body force (20) and Maxwell stress (21) vanish, and momentum balances reduce to those of classical continua. With these reductions, the term in parentheses in (34) still vanishes, and the final form of the energy balance (35), remains unchanged. However, the stress tensor is now symmetric, and hence the skew part of the velocity gradient does not contribute to the rate of change of internal energy.

Different contributions to the energy balance from electromechanical non-linearity are suggested in different theories [27,50,58,59]; the local balance (35) matches that of Tiersten [58] except for Tiersten's use of polarization per unit mass rather than the polarization per unit volume. Polarization gradients may be important for describing some physical phenomena [10,49,52]; in such

cases, augmentation of the energy balance to account for effects of polarization gradients may be necessary.

2.5. Entropy production

The global form of the Clausius–Duhem inequality is written [45,50,58]

$$\frac{d}{dt}\int_v \rho\eta \, dv \geqslant \int_v \frac{\rho r}{\theta} \, dv - \int_s \frac{\langle \mathbf{q}^-, \mathbf{n}\rangle}{\theta} \, ds, \tag{36}$$

where η is the entropy per unit mass and $\theta(\mathbf{X}, t)$ is the temperature. Application of the divergence theorem and differentiation of the Helmholtz free energy $\psi = e - \theta\eta$ provides a local form of (36)

$$\rho(\dot{e} - \dot{\psi} - \dot{\theta}\eta - r) + \langle \overset{\mathbf{g}}{\nabla}, \mathbf{q}\rangle - \frac{1}{\theta}\langle \overset{\mathbf{g}}{\nabla}\theta, \mathbf{q}\rangle \geqslant 0. \tag{37}$$

The entropy production inequality following from insertion of (35) into (37) is

$$\langle \boldsymbol{\sigma}, \mathbf{D}\rangle - \langle \boldsymbol{\sigma}, \mathbf{W}\rangle + \langle \hat{\mathbf{e}}, \dot{\hat{\mathbf{p}}}\rangle - \rho(\dot{\psi} + \dot{\theta}\eta) - \frac{1}{\theta}\langle \overset{\mathbf{g}}{\nabla}\theta, \mathbf{q}\rangle \geqslant 0, \tag{38}$$

where the covariant velocity gradient $\mathbf{L}$ is decomposed into a symmetric part $\mathbf{D}$ and skew part $\mathbf{W}$.

3. Elastic dielectric solids

Elastic dielectrics considered in the present section contain no defects. Such materials obey the Cauchy–Born hypothesis [6,26], that is, both the material and the primitive Bravais lattice vectors of the crystal structure deform via the deformation gradient $\mathbf{F}$ of (1). Under a homogeneous deformation in the sense of Born and Huang [6], a polarized dielectric may also exhibit a relative translation among different atomic species (e.g., positive and negative ions) comprising the basis of the crystal structure. The current Section provides a point of reference for comparison with the theory for defective crystals developed later in Section 4.

3.1. Constitutive assumptions

Constitutive functions are first assumed to exhibit the following dependencies, prior to consideration of objectivity requirements:

$$\psi = \psi(\mathbf{F}, \hat{\mathbf{p}}, \theta), \quad \eta = \eta(\mathbf{F}, \hat{\mathbf{p}}, \theta), \quad \boldsymbol{\sigma} = \boldsymbol{\sigma}(\mathbf{F}, \hat{\mathbf{p}}, \theta), \quad \hat{\mathbf{e}} = \hat{\mathbf{e}}(\mathbf{F}, \hat{\mathbf{p}}, \theta),$$

$$\mathbf{q} = \mathbf{q}(\mathbf{F}, \hat{\mathbf{p}}, \theta, \overset{\mathbf{g}}{\nabla}\theta). \tag{39}$$

Use of polarization as an independent state variable and electric field as a dependent variable follows general schemes of Devonshire [20] and Toupin [59]. The choice of electric field as independent variable and polarization as dependent variable is also possible [22,50,60]. Via (6), the electric displacement $\hat{\mathbf{d}}$ could substitute for either of the electric field or polarization in the thermodynamic potentials.

Consider rigid body motions of the form $\mathbf{x} \to \hat{\mathbf{Q}}\mathbf{x} + \mathbf{c}$, where $\hat{\mathbf{Q}} = \hat{\mathbf{Q}}^{-T}$ is a constant rotation tensor and $\mathbf{c}$ is a constant translation vector. Under such motions, spatial polarization and electric field vectors transform as $\hat{\mathbf{p}} \to \hat{\mathbf{Q}}\hat{\mathbf{p}}$ and $\hat{\mathbf{e}} \to \hat{\mathbf{Q}}\hat{\mathbf{e}}$, and the remaining non-scalar variables in (39) transform according to $\mathbf{F} \to \hat{\mathbf{Q}}\mathbf{F}$, $\boldsymbol{\sigma} \to \hat{\mathbf{Q}}\boldsymbol{\sigma}\hat{\mathbf{Q}}^T$, $\mathbf{q} \to \hat{\mathbf{Q}}\mathbf{q}$, and $\theta^a \to \hat{Q}^a_{.b}\theta^b$. On the other hand, the referential polarization and electric field vectors are invariant under rigid body motions

$$\hat{\mathbf{P}} = \mathbf{F}^T\hat{\mathbf{p}} \to \mathbf{F}^T\hat{\mathbf{Q}}^T\hat{\mathbf{Q}}\hat{\mathbf{p}} = \hat{\mathbf{P}}, \quad \hat{\mathbf{E}} = \mathbf{F}^T\hat{\mathbf{e}} \to \mathbf{F}^T\hat{\mathbf{Q}}^T\hat{\mathbf{Q}}\hat{\mathbf{e}} = \hat{\mathbf{E}}, \tag{40}$$

and thus are valid candidates for use in frame-indifferent constitutive relations. The following objective forms of (39) are suggested:

$$\psi = \psi(\mathbf{E}, \hat{\mathbf{P}}, \theta), \quad \eta = \eta(\mathbf{E}, \hat{\mathbf{P}}, \theta) \quad \boldsymbol{\Sigma} = \boldsymbol{\Sigma}(\mathbf{E}, \hat{\mathbf{P}}, \theta), \quad \hat{\mathbf{E}} = \hat{\mathbf{E}}(\mathbf{E}, \hat{\mathbf{P}}, \theta),$$

$$\mathbf{Q} = \mathbf{Q}(\mathbf{E}, \hat{\mathbf{P}}, \theta, \overset{\mathbf{G}}{\nabla}\theta). \tag{41}$$

with reference heat flux $\mathbf{Q} = J\mathbf{F}^{-1}\mathbf{q}$, second Piola–Kirchhoff stress—possibly non-symmetric with components $\Sigma^{AB} = JF^{-1A}_{.a}\sigma^{ab}F^{-1B}_{.b}$—and reference temperature gradient $\overset{G}{\nabla}_A\theta = F^a_{.A}\overset{g}{\nabla}_a\theta$ all remaining unchanged under rigid rotations [17].

3.2. Thermodynamics

The stress power entering (35) and (38) can be written as

$$\sigma^{ab}L_{ab} = J^{-1}(JF^{-1A}_{.b}\sigma^{cb}g_{ac})\dot{F}^a_{.A} = J^{-1}P^A_a\dot{F}^a_{.A}, \tag{42}$$

where $\mathbf{P}$ is the first Piola–Kirchhoff stress. Expanding the rate of free energy using (39) gives

$$\dot{\psi} = \left\langle \frac{\partial\psi}{\partial\mathbf{E}}, \dot{\mathbf{E}}\right\rangle + \left\langle \frac{\partial\psi}{\partial\hat{\mathbf{P}}}, \dot{\hat{\mathbf{P}}}\right\rangle + \frac{\partial\psi}{\partial\theta}\dot{\theta}, \tag{43}$$

where

$$\frac{\partial\psi}{\partial E_{AB}}\dot{E}_{AB} = F^a_A\frac{\partial\psi}{\partial E_{AB}}g_{ab}\dot{F}^b_{.B}, \quad \frac{\partial\psi}{\partial\hat{P}_A}\dot{\hat{P}}_A = \frac{\partial\psi}{\partial\hat{P}_A}\hat{p}_a\dot{F}^a_{.A} + \frac{\partial\psi}{\partial\hat{P}_A}F^a_A\dot{\hat{p}}_a. \tag{44}$$

Substitution of (42)–(44) into dissipation inequality (38) then leads to

$$\left\langle J^{-1}\mathbf{P} - \rho\mathbf{g}\mathbf{F}\frac{\partial\psi}{\partial\mathbf{E}} - \rho\hat{\mathbf{P}}\mathbf{F}^{-1}\otimes\frac{\partial\psi}{\partial\hat{\mathbf{P}}}, \dot{\mathbf{F}}\right\rangle + \left\langle \hat{\mathbf{e}} - \rho\mathbf{F}\frac{\partial\psi}{\partial\hat{\mathbf{P}}}, \dot{\hat{\mathbf{p}}}\right\rangle - \rho\left(\frac{\partial\psi}{\partial\theta} + \eta\right)\dot{\theta}$$

$$- J^{-1}\theta^{-1}\left\langle \overset{\mathbf{G}}{\nabla}\theta, \mathbf{Q}\right\rangle \geqslant 0. \tag{45}$$

Consider first isothermal conditions for which temperature rates and temperature gradients vanish. Under such conditions, presuming that the dissipation must remain non-negative when either the rate of spatial polarization or the rate of deformation gradient assumes an arbitrary value, the following constitutive relationships follow from (45):

$$\hat{\mathbf{E}} = \mathbf{C}\rho\frac{\partial\psi}{\partial\hat{\mathbf{P}}}, \quad \hat{E}_A = C_{AB}\rho\frac{\partial\psi}{\partial\hat{P}_B}, \tag{46}$$

$$\mathbf{P} = \rho_0\left(\mathbf{F}\frac{\partial\psi}{\partial\mathbf{E}} + \hat{\mathbf{P}}\mathbf{F}^{-1}\otimes\frac{\partial\psi}{\partial\hat{\mathbf{P}}}\right), \quad P^{aA} = \rho_0\left(F^a_{.B}\frac{\partial\psi}{\partial E_{BA}} + g^{ab}\hat{P}_B F^{-1B}_{.b}\frac{\partial\psi}{\partial\hat{P}_A}\right). \tag{47}$$

Substituting (46) into (47), second Piola–Kirchhoff and Cauchy stresses become, respectively,

$$\Sigma^{AB} = F^{-1A}_{.a}P^{aB} = \rho_0\frac{\partial\psi}{\partial E_{AB}} + JC^{-1AC}\hat{P}_C C^{-1BD}\hat{E}_D,$$

$$\sigma^{ab} = J^{-1}F^a_{.A}\Sigma^{AB}F^b_{.B} = 2\rho\frac{\partial\psi}{\partial g_{ab}} + \hat{p}^a\hat{e}^b, \tag{48}$$

where $C^{-1AB} = F^{-1A}_{.b}g^{ab}F^{-1B}_{.b}$. The second terms on each of the right sides of (48) account for possibly non-symmetric parts of the stress tensors. These terms arise from second-order electromechanical interactions. Consistency of skew-symmetric parts of (27) and (48) is revealed by $\sigma^{[ab]} = \hat{e}^{[b}\hat{p}^{a]} = \hat{\tau}^{[ba]}$, and the symmetric total stress is

$$\boldsymbol{\tau} = 2\rho\frac{\partial\psi}{\partial\mathbf{g}} + \hat{\mathbf{p}}\otimes\hat{\mathbf{e}} + \hat{\mathbf{e}}\otimes\hat{\mathbf{p}} + \varepsilon_0\hat{\mathbf{e}}\otimes\hat{\mathbf{e}} - \frac{\varepsilon_0}{2}(\hat{\mathbf{e}}\cdot\hat{\mathbf{e}})\mathbf{g}^{-1}. \tag{49}$$

The first term on the right of (49) is recognizable as the Doyle–Ericksen formula for hyperelastic solids [23,47]. The final two terms in (49) contribute to electrostriction, even in non-polar solids. Presuming that (45)–(47) must hold in the absence of temperature gradients

$$\eta = -\frac{\partial\psi}{\partial\theta}. \tag{50}$$

The entropy inequality thus reduces to the heat conduction inequality. When a referential version of Fourier's Law applies, then

$$\mathbf{Q} = -\mathbf{K} \overset{\mathbf{G}}{\nabla} \theta, \quad Q^A = -K^{AB}\theta_{,B}, \tag{51}$$

where the conductivity $\mathbf{K}$ is symmetric and positive semi-definite such that $-Q^A\theta_{,A} = K^{AB}\theta_{,A}\theta_{,B} \geqslant 0$.

The energy balance (35) is now revisited. The specific heat capacity c is introduced, from (50) satisfying

$$c = \frac{\partial e}{\partial \theta} = \frac{\partial e}{\partial \eta}\frac{\partial \eta}{\partial \theta} = -\theta\frac{\partial^2\psi}{\partial\theta^2}. \tag{52}$$

Using (42)–(51) and multiplying spatial energy balance (35) by J gives

$$-\theta\frac{d}{dt}\left(\rho_0\frac{\partial\psi}{\partial\theta}\right) = \rho_0\theta\dot{\eta} = \langle\overset{\mathbf{G}}{\nabla}, \mathbf{K}\overset{\mathbf{G}}{\nabla}\theta\rangle + \rho_0 r. \tag{53}$$

Carrying out the time derivative using (43) and substituting with (52) results in

$$-\theta\frac{d}{dt}\left(\rho_0\frac{\partial\psi}{\partial\theta}\right) = -\rho_0\theta\left(\frac{\partial\dot\psi}{\partial\theta}\right) = \rho_0 c\dot\theta + \theta\langle\boldsymbol{\beta}, \dot{\mathbf{E}}\rangle + \theta\langle\boldsymbol{\chi}, \dot{\hat{\mathbf{P}}}\rangle, \tag{54}$$

where the cross-derivatives account for thermoelastic and thermoelectric coupling, respectively,

$$\boldsymbol{\beta} = -\rho_0\frac{\partial^2\psi}{\partial\theta\,\partial\mathbf{E}}, \quad \boldsymbol{\chi} = -\rho_0\frac{\partial^2\psi}{\partial\theta\,\partial\hat{\mathbf{P}}}. \tag{55}$$

Equating (53) and (54), a rate equation for the temperature emerges

$$\rho_0 c\dot\theta = \langle\overset{\mathbf{G}}{\nabla}, \mathbf{K}\overset{\mathbf{G}}{\nabla}\theta\rangle - \theta[\langle\boldsymbol{\beta}, \dot{\mathbf{E}}\rangle + \langle\boldsymbol{\chi}, \dot{\hat{\mathbf{P}}}\rangle] + \rho_0 r, \tag{56}$$

with the first term on the right capturing heat conduction, the second and third terms capturing thermomechanical and thermoelectrical couplings, respectively, and the final term capturing non-mechanical sources of heat energy.

3.3. Representative free energy

Free energy function ψ in the first of (41) is examined in more detail for illustrative purposes. Consider the following form of the free energy per unit reference volume:

$$\rho_0\psi = \tfrac{1}{2}\mathbf{E} : \mathbb{C} : \mathbf{E} + \tfrac{1}{2}\langle\hat{\mathbf{P}}, \boldsymbol{\Lambda}\hat{\mathbf{P}}\rangle + \langle\hat{\mathbf{P}}, \boldsymbol{\Delta} : \mathbf{E}\rangle - (\theta - \theta_0)\boldsymbol{\beta} : \mathbf{E}$$
$$- (\theta - \theta_1)\langle\boldsymbol{\chi}, \hat{\mathbf{P}}\rangle + Y, \tag{57}$$

where the constant coefficients are

$$\mathbb{C} = \rho_0\frac{\partial^2\psi}{\partial\mathbf{E}\,\partial\mathbf{E}}\bigg|_{\substack{\mathbf{E}=\mathbf{0}\\ \hat{\mathbf{P}}=\mathbf{0}\\ \theta=\theta_0}}, \quad \boldsymbol{\Lambda} = \rho_0\frac{\partial^2\psi}{\partial\hat{\mathbf{P}}\,\partial\hat{\mathbf{P}}}\bigg|_{\substack{\mathbf{E}=\mathbf{0}\\ \hat{\mathbf{P}}=\mathbf{0}\\ \theta=\theta_0}}, \quad \boldsymbol{\Delta} = \rho_0\frac{\partial^2\psi}{\partial\hat{\mathbf{P}}\,\partial\mathbf{E}}\bigg|_{\substack{\mathbf{E}=\mathbf{0}\\ \hat{\mathbf{P}}=\mathbf{0}\\ \theta=\theta_0}},$$
$$\boldsymbol{\beta} = -\rho_0\frac{\partial^2\psi}{\partial\theta\,\partial\mathbf{E}}\bigg|_{\substack{\mathbf{E}=\mathbf{0}\\ \hat{\mathbf{P}}=\mathbf{0}\\ \theta=\theta_0}}, \quad \boldsymbol{\chi} = -\rho_0\frac{\partial^2\psi}{\partial\theta\,\partial\hat{\mathbf{P}}}\bigg|_{\substack{\mathbf{E}=\mathbf{0}\\ \hat{\mathbf{P}}=\mathbf{0}\\ \theta=\theta_1}}. \tag{58}$$

Here, $\mathbb{C}^{ABCD}$ are elastic moduli, Λ^{AB} are inverse dielectric susceptibilities, Δ^{ABC} are piezoelectric coefficients, and $Y = Y(\theta)$ is the thermal energy. The following symmetries emerge from (58):

$$\mathbb{C}^{ABCD} = \mathbb{C}^{CDAB} = \mathbb{C}^{BACD} = \mathbb{C}^{ABDC}, \quad \Lambda^{AB} = \Lambda^{BA}, \quad \beta^{AB} = \beta^{BA},$$
$$\Delta^{ABC} = \Delta^{ACB}, \tag{59}$$

meaning that the elastic moduli contain up to 21 independent coefficients, the dielectric susceptibilities and thermal stress parameters up to six independent coefficients, and the piezoelectric moduli up to 18 independent coefficients. The coefficients in (58) require

modification to accommodate more general non-linear behavior. For example, a coupled dependency of dielectric susceptibility on temperature and even powers of polarization is useful for describing energy wells and phase transitions in ferroelectric crystals [20] and variations in the dielectric constant with applied voltage [39]. Allowance of dielectric and piezoelectric coefficients to vary with polarization enables description of hysteresis under cyclic electric fields [64]. A term quadratic in polarization and linear in strain can be added to (57) to account for additional electrostriction [49].

The piezoelectric effect, $\Delta^{ABC} \neq 0$, is present in 20 of the 21 non-centrosymmetric crystal classes [19,43]. Of these, 10 crystal classes possess a unique polar axis and may exhibit polarization in the absence of applied electric fields and applied strains. In the context of (55), such materials possess a non-zero pyroelectric coefficient $\boldsymbol{\chi}$, leading to polarization with temperature variation.

4. Dielectrics with mobile vacancies

In what follows, the theory of non-linear elastic dielectrics of Section 3 is extended to account for vacancy defects, possibly mobile and possibly charged. Such a theory may be used to describe dielectric thin film devices containing mobile oxygen vacancies, for example [14–16,53] or silicon carbide with mobile C or Si vacancies [3], though it applies to more general scenarios as well (e.g. ceramics with point defects).

4.1. Governing equations

Maxwell's equations of electrostatics and balances of linear and angular momentum apply here, specifically local forms (10), (11), (23) and (27). However, the free charge density (5) is extended to delineate non-vanishing charges carried by vacancies in ionic solids from other charges, and the balance of energy and dissipation inequality are modified to account for electrochemical energy supplied by fluxes and rates of mobile vacancies. The global rate of energy exchange from thermochemical sources in (29) is generalized to include energy supplied by the vacancy flux

$$\mathscr{Q} = \int_v \rho r\, dv - \int_s \langle\mathbf{q}^-, \mathbf{n}\rangle\, ds - \int_s m^-\langle\boldsymbol{\zeta}^-, \mathbf{n}\rangle\, ds, \tag{60}$$

where $\boldsymbol{\zeta} \in T_x B$ is the flux of vacancies, with dimensions of velocity per unit spatial volume, and m is the scalar chemical potential,[2] with dimensions of energy. Equivalently, $\boldsymbol{\zeta}$ may be viewed as the number of vacancies traversing an oriented area element $\mathbf{n}\, ds$ per unit time and m the (electro)chemical energy carried per (charged) vacancy. The chemical potential can be associated with the energy required to move an atom from an interior lattice site to a lattice site on the surface, leaving behind a vacancy in the interior [34]. The vacancy flux is continuous across interfaces such that $\langle[\![\boldsymbol{\zeta}]\!], \mathbf{n}\rangle = 0$ along s. The sign convention follows that used for the heat flux $\mathbf{q}$, meaning that when m is positive, vacancies and energy flow out of the body when $m^-\langle\boldsymbol{\zeta}^-, \mathbf{n}\rangle > 0$ on s. When the contacting medium along s is impermeable to vacancies, $\langle\boldsymbol{\zeta}^-, \mathbf{n}\rangle = \langle\boldsymbol{\zeta}^+, \mathbf{n}\rangle = 0$. On the other hand, when the contacting medium along s is vacuum as opposed to another solid body, vacancies are annihilated as they flow from the dielectric body into the vacuum or are created as they flow from the vacuum into the dielectric body. It is important to note that m is not a constant, and instead may generally depend upon field variables such as stress, temperature, and charge density. For simplicity, only a single species of vacant atoms or ions is considered, meaning that each vacancy carries the same charge and occupies the

---

[2] More generally, a tensor chemical potential with components m^a_b could be used [7,31] so that the energy flux becomes $m^a_b\zeta^b n_a$. Here (60) is limited to isotropy, implying that $m^a_b = m\delta^a_b$.

same volume. Mass transport associated with movement of atoms between interstitial sites is not considered.

Let ξ denote the number of vacancies per unit spatial volume. The vacancy content of the body increases (decreases) only when vacancies enter (exit) at interfaces with other bodies or free surfaces. Internal generation and annihilation of vacancies are not considered. Hence, the global time rate of vacancies per unit volume in the body in the current configuration is dictated by the conservation law

$$\frac{d}{dt}\int_v \xi \, dv = -\int_s \langle \zeta^-, \mathbf{n} \rangle \, ds. \tag{61}$$

Relation (61) is mapped to the reference configuration as

$$\int_V \dot{\xi}_0 \, dV = -\int_S \langle \zeta_0^-, \mathbf{N} \rangle \, dS, \tag{62}$$

where $\xi_0 = J\xi$ and $\zeta_0 = J\mathbf{F}^{-1}\zeta$. Applying Gauss's theorem to (62) and localizing the result gives

$$\dot{\xi}_0 = -\langle \overset{\mathbf{G}}{\nabla}, \zeta_0 \rangle, \tag{63}$$

which enforces conservation of vacancies in the bulk solid [14,15,32].

It is assumed that electric charges may be carried by vacancies such that their contribution to the charge density in (5) is [14,15,36]

$$\hat{\rho}^V = ez\xi, \tag{64}$$

where z is an integer valence number. For vacant anion sites, $z > 0$, while for vacant cation sites, $z < 0$. The charge density (5) is modified as

$$\hat{\rho} = \hat{\rho}^C + \hat{\rho}^V = \sum_i \hat{n}^{(i)} ez^{(i)} + ez\xi, \tag{65}$$

where $\hat{\rho}^C$ is the density of electronic charges introduced in (5) and $\hat{\rho}^V$ accounts for the contribution of charged defects whose density may evolve with time via (61). Global charge conservation suggests that electronic charges contributing to $\hat{\rho}^C$ in (65) could vary with time in order to compensate for a non-zero rate of $\hat{\rho}^V$. However, because electronic charges travel much faster than diffusing vacancies, and because time scales of present interest correspond to those associated with vacancy diffusion, it is assumed that contributions from moving electronic charges (i.e., electric current) can be neglected in the governing equations, consistent with the quasi-electrostatic approximation. In other words, free charges are assumed to rapidly self-equilibrate [62]. With these assumptions, (63) is analogous to the proportionality relationship between the rate of free electronic charges and the negative divergence of an unsteady electric current in electrodynamics [49]. Note that $\hat{\rho}^V$ contributes to (11) and (20). Because the time rate of $\hat{\rho}^V$ may be non-zero, the local rate of electromechanical energy in (32) becomes

$$\Omega = [\dot{\hat{\phi}}_{,a} - \hat{\phi}_{,b}\overset{\mathbf{g}}{\nabla}_a v^b + \hat{\phi}_{,a}\overset{\mathbf{g}}{\nabla}_b v^b]\hat{d}^a + \frac{\varepsilon_0}{2}\hat{\phi}_{,a}\hat{\phi}^{,a}\overset{\mathbf{g}}{\nabla}_b v^b$$
$$- \hat{\phi}[\dot{\hat{\rho}}^V + \hat{\rho}^V\overset{\mathbf{g}}{\nabla}_b v^b], \tag{66}$$

where the final term on the right side accounts for the increase in total internal energy resulting from an evolving charge density associated with mobile vacancies.

From the divergence theorem, the chemical work associated with the final term on the right of (60) is

$$-\int_s m^-\langle \zeta^-, \mathbf{n} \rangle \, ds = -\int_v m\langle \overset{\mathbf{g}}{\nabla}, \zeta \rangle \, dv - \int_v \langle \overset{\mathbf{g}}{\nabla} m, \zeta \rangle \, dv. \tag{67}$$
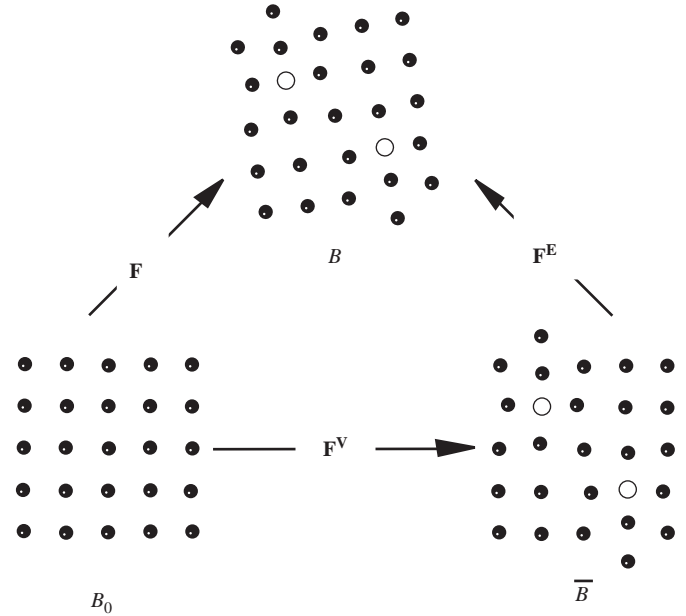

Fig. 2. Kinematic description of deforming crystal volume element of fixed mass; dark circles represent atoms and open circles represent vacancies.

Applying Piola's identity and (63) to the first integrand on the right of (67) results in

$$-m\langle \overset{\mathbf{g}}{\nabla}, \zeta \rangle = -J^{-1}m\langle \overset{\mathbf{G}}{\nabla}, \zeta_0 \rangle - m\langle \overset{\mathbf{g}}{\nabla} \bullet (J^{-1}\mathbf{F}), \zeta_0 \rangle = J^{-1}m\dot{\xi}_0$$
$$= m(\dot{\xi} + \xi tr\mathbf{L}). \tag{68}$$

Upon replacing the second of (29) with (60) and using (66) in place of (32), global energy balance (28) is consulted. Then, after appealing to (64), (67) and (68), the local balance of energy is expressed as

$$\rho\dot{e} = \langle \boldsymbol{\sigma}, \mathbf{L}^T \rangle - \langle \overset{\mathbf{g}}{\nabla}, \mathbf{q} \rangle + \rho r + \langle \hat{\mathbf{e}}, \dot{\hat{\mathbf{p}}} \rangle + m(\dot{\xi} + \xi tr\mathbf{L}) - \langle \overset{\mathbf{g}}{\nabla} m, \zeta \rangle$$
$$- ez\hat{\phi}(\dot{\xi} + \xi tr\mathbf{L}), \tag{69}$$

differing from (35) via the addition of the final three terms. These terms are associated with the chemical potential energy supplied by vacancy rates and fluxes and the electromechanical energy attributed to the time rate of change of charged vacancies. Substituting (69) into (37) provides the dissipation inequality for dielectrics with charged vacancies, referred to configuration B

$$\langle \boldsymbol{\sigma}, \mathbf{L}^T \rangle + \langle \hat{\mathbf{e}}, \dot{\hat{\mathbf{p}}} \rangle + m(\dot{\xi} + \xi tr\mathbf{L}) - \langle \overset{\mathbf{g}}{\nabla} m, \zeta \rangle - ez\hat{\phi}(\dot{\xi} + \xi tr\mathbf{L}) - \rho(\dot{\psi} + \dot{\theta}\eta)$$
$$- \frac{1}{\theta}\langle \overset{\mathbf{g}}{\nabla} \theta, \mathbf{q} \rangle \geqslant 0. \tag{70}$$

4.2. Kinematics

The deformation gradient of (1) is decomposed multiplicatively [4,44] to account for recoverable thermoelastic deformation $\mathbf{F^E}$ and volumetric deformation $\mathbf{F^V}$ attributed to vacancies

$$\mathbf{F} = \mathbf{F^E}\mathbf{F^V}, \quad F_A^a = F_{.\alpha}^{Ea}F_A^{V\alpha}, \tag{71}$$

implying the existence of an unstressed intermediate configuration [25] labeled in Fig. 2 as $\bar{B}$, and a corresponding series of global tangent mappings $\mathbf{F^V} : TB_0 \to T\bar{B}$ and $\mathbf{F^E} : T\bar{B} \to TB$ [4,13]. The elastic deformation $\mathbf{F^E}$ consists of stretch of the lattice due to mechanical loading, elastic and rigid body rotations, and deformation resulting from thermal expansion or contraction induced by temperature changes. The latter is considered reversible: in the absence of other deformation modes, restoration of the local crystal element to its

reference temperature relieves the thermal strain. Deformation from vacancies $\mathbf{F^V}$ is mechanically irreversible, since it generally remains when external forces are removed from the crystal, and is assumed to manifest only through a change in volume of the solid. Possible shape changes of the solid associated with non-spherical pores or anisotropic clusters of vacancies within a given volume element of crystal are not considered. Because the deformation resulting from vacancies is isotropic, it can be expressed as

$$\mathbf{F^V} = (1 - \bar{\phi})^{-1/3}\bar{\boldsymbol{\delta}}, \quad F_A^{V\alpha} = (1 - \bar{\phi})^{-1/3}\bar{\delta}_{.A}^{\alpha}. \tag{72}$$

The scalar

$$\bar{\phi} = (d\bar{V} - dV)/d\bar{V} = 1 - J^{V-1} \tag{73}$$

is the volume fraction of vacancies per unit volume in configuration $\bar{B}$ [2,13,42], where J^V is the Jacobian determinant of $\mathbf{F^V}$. Neither $\mathbf{F^E}$ nor $\mathbf{F^V}$ need be integrable to a displacement function; specifically, incompatibility of the latter is reflected by the quantity $\bar{\delta}_{.[A}^{\alpha}\bar{\phi}_{,B]}$, non-zero when the field $\bar{\phi}(\mathbf{X}, t)$ is heterogeneous. An external Cartesian coordinate frame with basis vectors not tangent to any material lines is implied for anholonomic configuration $\bar{B}$ [12], with corresponding Cartesian metric $\bar{g}_{\alpha\beta} = \delta_{\alpha\beta}$. Also, $\bar{\boldsymbol{\delta}}$ is the shifter between $\bar{B}$ and B_0, equivalent in (73) to the identity map $\mathbf{1}$ with coincident coordinate axes implied in $\bar{B}$ and B_0.

As illustrated in Fig. 2, the reference configuration is a perfect crystal, free from defects, though the theory does not preclude a distribution of vacancies at $t = 0$. Notice that by (72), vacancies increase the specific volume and decrease the mass density of an element of fixed mass when $\bar{\phi} > 0$. As shown in Fig. 2, the total number of atoms in the element under consideration remains fixed in all configurations, i.e. mass is conserved in agreement with (2). Introduction of a vacancy by removal of an atom from a perfect lattice site can cause contraction of the remaining atoms towards the defect such that the energy associated with interatomic separation distances is reduced, shown qualitatively by the local attraction of a few of the atoms to their neighboring vacant sites in Fig. 2. For example, according to continuum elasticity theory, the radial displacement field induced by a spherical point defect in an infinite isotropic body decays inversely to the square of the radial distance from the defect [28]. When the reduction in volume induced by such local displacement fields (i.e. the relaxation volume) is small compared to the volume associated with each vacant lattice site (i.e. the atomic volume), then $J^V > 1$. Otherwise, when the relaxation volume is larger than the atomic volume due to strong interatomic forces, $J^V < 1$ and $\bar{\phi} < 0$, and the overall volume per unit mass relative to a perfect crystal is reduced by vacancies. For ionic crystals, additional expansion or contraction resulting from electrostatic interactions between ions surrounding charged vacant sites is conceivable; such effects are embedded in $\mathbf{F^V}$. Charge neutrality need not occur in each volume element of fixed mass.

From (71) and (72), the deformation rate resulting from vacancy flux is

$$\mathbf{L^V} = \dot{\mathbf{F}}^{\mathbf{V}}\mathbf{F}^{\mathbf{V}-1} = \dot{\bar{\phi}}(3 - 3\bar{\phi})^{-1}\mathbf{1}. \tag{74}$$

Let $\phi_0 = \alpha\xi_0$ denote the fraction of vacancies per unit reference volume, where α is a scalar constant denoting the volume change effected by a single vacancy. Net expansion is represented by $\alpha > 0$, and net contraction by $\alpha < 0$. The following relationships then emerge between dimensionless volume fractions and number densities of vacancies:

$$\bar{\phi} = J^{V-1}\phi_0 = J^{V-1}\alpha\xi_0 = (1 - \bar{\phi})\alpha\xi_0 = J^E\alpha\xi, \tag{75}$$

where J^E is the Jacobian determinant of $\mathbf{F^E}$.

The following notation is introduced, to label variables couched in intermediate configuration $\bar{B}$, the configuration acting here as an evolving reference state for the thermoelastic response [11,25,44]:

$$\bar{\rho} = \rho_0 J^{V-1} = \rho J^E, \tag{76}$$

$$2\mathbf{E^E} = \mathbf{C^E} - \mathbf{1}, \quad C_{\alpha\beta}^E = F_{.\alpha}^{Ea}g_{ab}F_{.\beta}^{Eb}, \tag{77}$$

$$\bar{\boldsymbol{\Sigma}} = J^{V-1}\mathbf{F^V}\boldsymbol{\Sigma}\mathbf{F^{VT}} = J^E\mathbf{F^E}^{-1}\boldsymbol{\sigma}\mathbf{F^{E-T}}, \tag{78}$$

$$\bar{\nabla}\theta = (\overset{\mathbf{G}}{\nabla}\theta)\mathbf{F^{V-1}} = (\overset{\mathbf{g}}{\nabla}\theta)\mathbf{F^E}, \quad \bar{\nabla}m = (\overset{\mathbf{G}}{\nabla}m)\mathbf{F^{V-1}} = (\overset{\mathbf{g}}{\nabla}m)\mathbf{F^E}, \tag{79}$$

$$\bar{\mathbf{q}} = J^{V-1}\mathbf{F^V}\mathbf{Q} = J^E\mathbf{F^{E-1}}\mathbf{q}, \quad \bar{\boldsymbol{\zeta}} = J^{V-1}\mathbf{F^V}\boldsymbol{\zeta}_0 = J^E\mathbf{F^{E-1}}\boldsymbol{\zeta}, \tag{80}$$

$$\bar{\mathbf{p}} = \mathbf{F^{ET}}\hat{\mathbf{p}}, \quad \bar{\mathbf{e}} = \mathbf{F^{ET}}\hat{\mathbf{e}}, \quad \bar{\mathbf{d}} = J^E\mathbf{F^{E-1}}\hat{\mathbf{d}}. \tag{81}$$

The mass density per unit intermediate volume in $\bar{B}$ is written as $\bar{\rho}$ in (76). Introduced in (77) is the covariant elastic strain $\mathbf{E^E}$. In (78), relationships between contravariant elastic stress $\bar{\boldsymbol{\Sigma}} \in T\bar{B} \times T\bar{B}$, second Piola–Kirchhoff stress $\boldsymbol{\Sigma}$, and Cauchy stress $\boldsymbol{\sigma}$ are given. None of these stress measures need be symmetric in polarized media. The intermediate temperature gradient $\bar{\nabla}\theta$ and chemical potential gradient $\bar{\nabla}m$ follow in (79), where $\bar{\nabla}_\alpha = \overset{g}{\nabla}_a F_{.\alpha}^{Ea} = \overset{G}{\nabla}_A F_{.\alpha}^{V-1A}$ defines the anholonomic covariant derivative of a scalar function [13]. In (80), the heat flux and vacancy flux are each mapped from the reference to the intermediate configuration via appropriate Piola transformations. Polarization, electric field, and electric displacement are mapped to $\bar{B}$ according to (81); substitution into (6) then provides

$$\bar{\mathbf{d}} = J^{E-1}\mathbf{C^{E-1}}(\varepsilon_0\bar{\mathbf{e}} + \bar{\mathbf{p}}). \tag{82}$$

4.3. Constitutive assumptions

Constitutive functions used here are of the same form as (39), apart from five major differences that reflect the presence of inelastic deformation and defects. The first is that the recoverable thermoelastic strain $\mathbf{E^E}$, as opposed to the total strain $\mathbf{E}$, is used as an independent state variable, following the logic of multiplicative plasticity theory [11,44]. As such, the elastic stress $\bar{\boldsymbol{\Sigma}}$, work conjugate to $\mathbf{E^E}$, is used in place of the second Piola–Kirchhoff stress $\boldsymbol{\Sigma}$. The second is that electric field and polarization defined with respect to configuration $\bar{B}$ via (81) are used, as opposed to their referential counterparts $\hat{\mathbf{E}}$ and $\hat{\mathbf{P}}$. The third is that intermediate temperature gradient $\bar{\nabla}\theta$ of (79) and heat flux $\bar{\mathbf{q}}$ of (80) are used as opposed to analogous quantities defined on B_0. The fourth is that the response functions are assumed to depend upon the density of defects ξ, and the fifth is that a constitutive function for the vacancy flux is posited that, in addition to possibly depending on the other independent state variables, also depends upon the gradient of the chemical potential, $\bar{\nabla}m$. Constitutive functions are written generically as

$$\psi = \psi(\mathbf{E^E}, \bar{\mathbf{p}}, \xi, \theta), \quad \eta = \eta(\mathbf{E^E}, \bar{\mathbf{p}}, \xi, \theta), \quad \bar{\boldsymbol{\Sigma}} = \bar{\boldsymbol{\Sigma}}(\mathbf{E^E}, \bar{\mathbf{p}}, \xi, \theta), \quad \bar{\mathbf{e}} = \bar{\mathbf{e}}(\mathbf{E^E}, \bar{\mathbf{p}}, \xi, \theta),$$

$$\bar{\mathbf{q}} = \bar{\mathbf{q}}(\mathbf{E^E}, \bar{\mathbf{p}}, \xi, \theta, \bar{\nabla}\theta), \quad \bar{\boldsymbol{\zeta}} = \bar{\boldsymbol{\zeta}}(\mathbf{E^E}, \bar{\mathbf{p}}, \xi, \theta, \bar{\nabla}m). \tag{83}$$

Verification is straightforward that all variables in (83) remain invariant under rigid body motions of the form $\mathbf{x} \to \hat{\mathbf{Q}}\mathbf{x} + \mathbf{c}$ with $\mathbf{F^E} \to \hat{\mathbf{Q}}\mathbf{F^E}$. The dependence on number of defects per unit spatial volume ξ could alternatively be replaced by a dependence on the volume fraction of defects $\bar{\phi}$ via (75).

4.4. Thermodynamics

Use of (71)–(75) leads to the expansion of the spatial velocity gradient

$$\mathbf{L} = \dot{\mathbf{F}}^{\mathbf{E}}\mathbf{F}^{\mathbf{E}-1} + (\bar{A}/3)[\dot{\xi} + \xi tr(\dot{\mathbf{F}}^{\mathbf{E}}\mathbf{F}^{\mathbf{E}-1})]\mathbf{1}, \quad \bar{A} = J^E\alpha(1 - J^E\alpha\xi)^{-1}, \tag{84}$$

where the scalar $\bar{A}$ appears prominently in what follows. The stress power entering (69) and (70) can be written

$$\sigma^{ab}L_{ab} = (J^{E-1}\bar{P}_a^\alpha - \bar{A}p\xi F_{.a}^{E-1\alpha})\dot{F}_{.\alpha}^{Ea} - \bar{A}p\dot{\xi}, \tag{85}$$

where $\bar{P}^{a\alpha} = J^E F_{.b}^{E-1}\sigma^{ab}$ is the elastic first Piola–Kirchhoff stress, and $p = -\sigma_{.a}^a/3$ is the Cauchy pressure. Expanding the rate of free energy from (83)

$$\dot{\psi} = \left\langle \frac{\partial \psi}{\partial \mathbf{E}^{\mathbf{E}}}, \dot{\mathbf{E}}^{\mathbf{E}} \right\rangle + \left\langle \frac{\partial \psi}{\partial \bar{\mathbf{p}}}, \dot{\bar{\mathbf{p}}} \right\rangle + \frac{\partial \psi}{\partial \theta}\dot{\theta} + \frac{\partial \psi}{\partial \xi}\dot{\xi}, \tag{86}$$

where from definitions (77) and (81)

$$\frac{\partial \psi}{\partial E_{\alpha\beta}^E}\dot{E}_{\alpha\beta}^E = F_{.\beta}^{Eb}\frac{\partial \psi}{\partial E_{\alpha\beta}^E}g_{ab}\dot{F}_{.\alpha}^{Ea}, \quad \frac{\partial \psi}{\partial \bar{p}_\alpha}\dot{\bar{p}}_\alpha = \frac{\partial \psi}{\partial \bar{p}_\alpha}\hat{p}_a\dot{F}_{.\alpha}^{Ea} + \frac{\partial \psi}{\partial \bar{p}_\alpha}F_{.\alpha}^{Ea}\dot{\hat{p}}_a. \tag{87}$$

Notice also that from (84)

$$\xi\,tr\mathbf{L} = \xi(1 + \bar{A}\xi)F_{.a}^{E-1\alpha}\dot{F}_{.\alpha}^{Ea} + \bar{A}\xi\dot{\xi}. \tag{88}$$

Substituting (84)–(88) into dissipation inequality (70) then yields

$$\begin{aligned}
&\left[J^{E-1}\bar{P}_a^\alpha - \bar{A}p\xi F_{.a}^{E-1\alpha} - \rho F_{.\beta}^{Eb}\frac{\partial \psi}{\partial E_{\alpha\beta}^E}g_{ab} - \rho\frac{\partial \psi}{\partial \bar{p}_\alpha}\hat{p}_a - ez\hat{\phi}\xi(1+\bar{A}\xi)F_{.a}^{E-1\alpha}\right. \\
&\left. + m\xi(1+\bar{A}\xi)F_{.a}^{E-1\alpha}\right]\dot{F}_{.\alpha}^{Ea} + \left[m(1+\bar{A}\xi) - ez\hat{\phi}(1+\bar{A}\xi) - \bar{A}p - \rho\frac{\partial \psi}{\partial \xi}\right]\dot{\xi} \\
&+ \left[\hat{e}^a - \rho\frac{\partial \psi}{\partial \bar{p}_\alpha}F_{.\alpha}^{Ea}\right]\dot{\hat{p}}_a - \left[\rho\frac{\partial \psi}{\partial \theta} + \eta\right]\dot{\theta} \\
&- J^{E-1}\theta^{-1}\bar{\nabla}_\alpha\theta\bar{q}^\alpha - J^{E-1}\bar{\nabla}_\alpha m\bar{\zeta}^\alpha \geqslant 0.
\end{aligned} \tag{89}$$

Consideration of distinct thermodynamic processes in conjunction with (89) leads to a number of constitutive laws [10,17,30,50]. Presuming that (89) must be satisfied for arbitrary rates of temperature leads to the usual relationship between temperature and entropy, identical to (50). Presuming that dissipation associated with the rate of polarization must be non-negative for arbitrary rates of polarization leads to

$$\hat{e}^a = F_{.\alpha}^{Ea}\rho\frac{\partial \psi}{\partial \bar{p}_\alpha}, \quad \bar{e}_\alpha = C_{\alpha\beta}^E\rho\frac{\partial \psi}{\partial \bar{p}_\beta}. \tag{90}$$

Assuming that dissipation associated with the rate of vacancy concentration must remain non-negative for arbitrary concentration rates in the absence of gradients in chemical potential or temperature, chemical potential m should satisfy

$$m = (1+\bar{A}\xi)^{-1}\rho\frac{\partial \psi}{\partial \xi} + ez\hat{\phi} + \bar{A}(1+\bar{A}\xi)^{-1}p. \tag{91}$$

Requiring non-negative dissipation associated with the elastic deformation gradient rate then gives

$$J^{E-1}\bar{P}_a^\alpha = \rho F_{.\beta}^{Eb}\frac{\partial \psi}{\partial E_{\alpha\beta}^E}g_{ab} + \bar{A}p\xi F_{.a}^{E-1\alpha} + \rho\frac{\partial \psi}{\partial \bar{p}_\alpha}\hat{p}_a + ez\hat{\phi}\xi(1+\bar{A}\xi)F_{.a}^{E-1\alpha} - m\xi(1+\bar{A}\xi)F_{.a}^{E-1\alpha}, \tag{92}$$

which upon substitution of (91) becomes

$$\bar{P}_a^\alpha = g_{ab}F_{.\beta}^{Eb}\bar{\rho}\frac{\partial \psi}{\partial E_{\alpha\beta}^E} + \hat{p}_a\bar{\rho}\frac{\partial \psi}{\partial \bar{p}_\alpha} - \xi F_{.a}^{E-1\alpha}\bar{\rho}\frac{\partial \psi}{\partial \xi}. \tag{93}$$

Using (90), the elastic stress and Cauchy stress are then, respectively,

$$\bar{\Sigma}^{\alpha\beta} = F_{.a}^{E-1\alpha}\bar{P}^{a\beta} = \bar{\rho}\frac{\partial \psi}{\partial E_{\alpha\beta}^E} + J^E C^{E-1\alpha\chi}\bar{p}_\chi C^{E-1\beta\delta}\bar{e}_\delta - \xi C^{E-1\alpha\beta}\bar{\rho}\frac{\partial \psi}{\partial \xi}, \tag{94}$$

$$\sigma^{ab} = J^{E-1}F_{.\alpha}^{Ea}\bar{\Sigma}^{\alpha\beta}F_{.\beta}^{Eb} = 2\rho\frac{\partial \psi}{\partial g_{ab}} + \hat{p}^a\hat{e}^b - \xi\rho\frac{\partial \psi}{\partial \xi}g^{ab}. \tag{95}$$

The final terms on the right of each of (94) and (95) account for possible effects of vacancy concentration on hydrostatic pressure. From (95), consistency of skew-symmetric parts of Cauchy and Maxwell stresses in (27) is revealed by $\sigma^{[ab]} = \hat{e}^{[b}\hat{p}^{a]} = \hat{\tau}^{[ba]}$, and the total stress is thus symmetric

$$\boldsymbol{\tau} = 2\rho\frac{\partial \psi}{\partial \mathbf{g}} + \xi\rho\frac{\partial \psi}{\partial \xi}\mathbf{g}^{-1} + \hat{\mathbf{p}}\otimes\hat{\mathbf{e}} + \hat{\mathbf{e}}\otimes\hat{\mathbf{p}} + \varepsilon_0\hat{\mathbf{e}}\otimes\hat{\mathbf{e}} - \frac{\varepsilon_0}{2}(\hat{\mathbf{e}}\cdot\hat{\mathbf{e}})\mathbf{g}^{-1}. \tag{96}$$

The remaining terms in dissipation inequality (89), upon consultation of (90)–(92), are

$$-J^{E-1}\theta^{-1}\langle\bar{\nabla}\theta,\bar{\mathbf{q}}\rangle - J^{E-1}\langle\bar{\nabla}m,\bar{\zeta}\rangle \geqslant 0. \tag{97}$$

Though more general formulations are possible, the contribution from the flux of thermal energy is non-negative when Fourier-type behavior occurs in the elastically unloaded configuration, analogous to (51)

$$\bar{\mathbf{q}} = -\bar{\mathbf{K}}\bar{\nabla}\theta, \quad (\bar{\nabla}_\alpha\theta)\bar{K}^{\alpha\beta}(\bar{\nabla}_\beta\theta) \geqslant 0, \tag{98}$$

where thermal conductivity matrix $\bar{\mathbf{K}} \in T\bar{B} \times T\bar{B}$ is symmetric and positive semi-definite. Analogously, the contribution to entropy production from the flux of vacancies can be made non-negative by assuming

$$\bar{\zeta} = -\bar{\mathbf{D}}\bar{\nabla}m, \quad (\bar{\nabla}_\alpha m)\bar{D}^{\alpha\beta}(\bar{\nabla}_\beta m) \geqslant 0, \tag{99}$$

with diffusivity matrix $\bar{\mathbf{D}} \in T\bar{B} \times T\bar{B}$ symmetric and positive semi-definite. Applying (98) and (99) in (97), the dissipation inequality is always satisfied:

$$(J^E\theta)^{-1}\langle\bar{\nabla}\theta,\bar{\mathbf{K}}\bar{\nabla}\theta\rangle + J^{E-1}\langle\bar{\nabla}m,\bar{\mathbf{D}}\bar{\nabla}m\rangle \geqslant 0. \tag{100}$$

Finally, from the form of the chemical potential in (91), the vacancy flux in (99) satisfies

$$\begin{aligned}
\bar{\zeta}^\alpha = -\bar{D}^{\alpha\beta}&\left\{\bar{\nabla}_\beta\left[(1+\bar{A}\xi)^{-1}\rho\frac{\partial \psi}{\partial \xi}\right] + ez\bar{\nabla}_\beta\hat{\phi}\right. \\
&\left.+ \bar{\nabla}_\beta\left[\bar{A}(1+\bar{A}\xi)^{-1}p\right]\right\}.
\end{aligned} \tag{101}$$

The first term on the right of (101) represents effects of concentration gradients on the flux of neutral or charged vacancies, the second represents effects of electrostatic potential gradients on the flux of charged vacancies, and the third term represents effects of pressure gradients on the flux of neutral or charged vacancies. Effects of gradients of concentration and pressure on diffusion are well documented [33,34,38], as are effects of gradients of electrostatic potential in ionic crystals [18,37,40,63].

4.5. Representative free energy

Further insight is achieved by considering a free energy per unit intermediate volume of the form

$$\begin{aligned}
\bar{\rho}\psi = \tfrac{1}{2}\mathbf{E}^{\mathbf{E}}\colon\bar{\mathbb{C}}:\mathbf{E}^{\mathbf{E}} + \tfrac{1}{2}\langle\bar{\mathbf{p}},\bar{\mathbf{\Lambda}}\bar{\mathbf{p}}\rangle + \langle\bar{\mathbf{p}},\bar{\Delta}:\mathbf{E}^{\mathbf{E}}\rangle \\
+ \tfrac{1}{2}\bar{\upsilon}\xi^2 - (\theta-\theta_0)\bar{\boldsymbol{\beta}}:\mathbf{E}^{\mathbf{E}} - (\theta-\theta_1)\langle\bar{\boldsymbol{\chi}},\bar{\mathbf{p}}\rangle - \bar{\rho}\bar{c}\theta\ln\left(\frac{\theta}{\theta_0}\right),
\end{aligned} \tag{102}$$

where θ_0 and θ_1 are constants with dimensions of temperature. The remaining coefficients in (102) are isothermal constants defined according to

$$\bar{\mathbb{C}} = \bar{\rho}\frac{\partial^2 \psi}{\partial \mathbf{E}^{\mathbf{E}}\partial \mathbf{E}^{\mathbf{E}}}\bigg|_{\substack{\mathbf{E}^{\mathbf{E}}=\mathbf{0}\\\bar{\mathbf{p}}=\mathbf{0}\\\xi=0\\\theta=\theta_0}}, \quad \bar{\mathbf{\Lambda}} = \bar{\rho}\frac{\partial^2 \psi}{\partial \bar{\mathbf{p}}\,\partial \bar{\mathbf{p}}}\bigg|_{\substack{\mathbf{E}^{\mathbf{E}}=\mathbf{0}\\\bar{\mathbf{p}}=\mathbf{0}\\\xi=0\\\theta=\theta_0}}, \quad \bar{\mathbf{\Delta}} = \bar{\rho}\frac{\partial^2 \psi}{\partial \bar{\mathbf{p}}\,\partial \mathbf{E}^{\mathbf{E}}}\bigg|_{\substack{\mathbf{E}^{\mathbf{E}}=\mathbf{0}\\\bar{\mathbf{p}}=\mathbf{0}\\\xi=0\\\theta=\theta_0}},$$

$$\bar{\upsilon} = \bar{\rho}\frac{\partial^2 \psi}{\partial \xi^2}\bigg|_{\substack{\mathbf{E^E}=\mathbf{0}\\ \bar{\mathbf{p}}=\mathbf{0}\\ \xi=0\\ \theta=\theta_0}}, \quad \bar{\boldsymbol{\beta}} = -\bar{\rho}\frac{\partial^2 \psi}{\partial \theta\, \partial \mathbf{E^E}}\bigg|_{\substack{\mathbf{E^E}=\mathbf{0}\\ \bar{\mathbf{p}}=\mathbf{0}\\ \xi=0\\ \theta=\theta_0}}, \quad \bar{\boldsymbol{\chi}} = -\bar{\rho}\frac{\partial^2 \psi}{\partial \theta\, \partial \bar{\mathbf{p}}}\bigg|_{\substack{\mathbf{E^E}=\mathbf{0}\\ \bar{\mathbf{p}}=\mathbf{0}\\ \xi=0\\ \theta=\theta_1}},$$

$$\bar{c} = -\theta\frac{\partial^2 \psi}{\partial \theta^2}\bigg|_{\substack{\mathbf{E^E}=\mathbf{0}\\ \bar{\mathbf{p}}=\mathbf{0}\\ \xi=0\\ \theta=\theta_0}}. \tag{103}$$

Terms in (102) referred to the intermediate configuration are analogous to those of the theory for elastic dielectrics in (57) referred to the reference configuration, apart from the quadratic form of the vacancy energy, $\bar{\upsilon}\xi^2/2$, that is newly introduced in (102). Consequences of this particular choice of vacancy energy with regards to diffusion are examined in more detail in Section 4.6. Arguments regarding symmetry analogous to (59) apply here as well.

From (94) and (102), the elastic stress is

$$\bar{\Sigma}^{\alpha\beta} = \bar{\mathbb{C}}^{\alpha\beta\chi\delta}E_{\chi\delta}^{E} + \bar{p}_{\chi}\bar{\varDelta}^{\chi\alpha\beta} - (\theta-\theta_0)\bar{\beta}^{\alpha\beta} - C^{E-1\alpha\beta}\bar{\upsilon}\xi^2$$
$$+ J^E C^{E-1\alpha\chi}\bar{p}_{\chi}C^{E-1\beta\delta}\bar{e}_{\delta}, \tag{104}$$

where the first four terms on the right side are symmetric contributions. The first term on the right side accounts for hyperelasticity, the second term accounts for the inverse piezoelectric effect, the third accounts for the thermoelastic effect (i.e. thermal expansion or contraction), the fourth accounts for vacancies, and the final term reflects the possibly non-symmetric contribution of the Maxwell stress. When the vacancy concentration is small and $\xi^2 \to 0$, the contribution of vacancies to the stress from the fourth term on the right of (104) is negligible. On the other hand, consider cases when this term is significant, when $\bar{\upsilon} > 0$, and when the elastic strain is held fixed. Under such constraints, the concentration of vacancies induces a negative hydrostatic component of $\bar{\Sigma}$, or a positive hydrostatic pressure.

From (90) and (102), the electric field referred to the intermediate configuration is

$$\bar{e}_{\alpha} = J^{E-1}C_{\alpha\beta}^{E}[\bar{\varLambda}^{\beta\chi}\bar{p}_{\chi} + \bar{\varDelta}^{\beta\chi\delta}E_{\chi\delta}^{E} - (\theta-\theta_1)\bar{\chi}^{\beta}]. \tag{105}$$

The first term in braces on the right side of (105) accounts for the dielectric permittivity, the second accounts for the piezoelectric effect, and the third term accounts for the pyroelectric effect. From (82)

$$\bar{d}^{\beta} = (\varepsilon_0\bar{\varLambda}^{\beta\chi} + J^E C^{E-1\beta\chi})\bar{p}_{\chi} + \bar{\varDelta}^{\beta\chi\delta}E_{\chi\delta}^{E} - (\theta-\theta_1)\bar{\chi}^{\beta}. \tag{106}$$

Assuming that $\bar{\varLambda}^{\alpha\beta}$ is positive definite and inverting (105)

$$\bar{p}_{\chi} = (J^E\bar{\varLambda}_{\chi\beta}^{-1}C^{E-1\beta\alpha})\bar{e}_{\alpha} - (\bar{\varLambda}_{\chi\beta}^{-1}\bar{\varDelta}^{\beta\delta\varepsilon})E_{\delta\varepsilon}^{E} + (\theta-\theta_1)(\bar{\varLambda}_{\chi\beta}^{-1}\bar{\chi}^{\beta})$$
$$= \widehat{\varLambda}_{\chi}{}^{\cdot\alpha}\bar{e}_{\alpha} - \widehat{\varDelta}_{\chi}{}^{\cdot\delta\varepsilon}E_{\delta\varepsilon}^{E} + (\theta-\theta_1)\widehat{\chi}_{\chi}, \tag{107}$$

where $\widehat{\boldsymbol{\Lambda}}$ depends on the elastic strain and where $\widehat{\Delta}$ and $\widehat{\chi}$ are constants. Substitution of (107) into (106) then yields the relationship between electric displacement and electric field

$$\bar{d}^{\beta} = [\varepsilon_0 J^E C^{E-1\beta\alpha} + J^{E2}C^{E-1\beta\chi}\bar{\varLambda}_{\chi\delta}^{-1}C^{E-1\delta\alpha}]\bar{e}_{\alpha} - [(\varepsilon_0-1)\bar{\varDelta}^{\beta\delta\varepsilon}$$
$$+ J^E C^{E-1\beta\chi}\bar{\varLambda}_{\chi\phi}^{-1}\bar{\varDelta}^{\phi\delta\varepsilon}]E_{\delta\varepsilon}^{E} + [(\varepsilon_0-1)\bar{\chi}^{\beta} + J^E C^{E-1\beta\chi}\bar{\varLambda}_{\chi\delta}^{-1}\bar{\chi}^{\delta}](\theta-\theta_1)$$
$$= \varepsilon_0\bar{\varepsilon}_R^{\beta\alpha}\bar{e}_{\alpha} - \hat{\varDelta}^{\beta\delta\varepsilon}E_{\delta\varepsilon}^{E} + \hat{\chi}^{\beta}(\theta-\theta_1), \tag{108}$$

where $\bar{\varepsilon}_R^{\alpha\beta} = J^E C^{E-1\alpha\beta} + \varepsilon_0^{-1}J^{E2}C^{E-1\alpha\chi}\bar{\varLambda}_{\chi\delta}^{-1}C^{E-1\delta\beta}$ is the relative permittivity and is clearly symmetric, and where the other notation is evident from (108). The first term on the right of (108), $\varepsilon_0\boldsymbol{\varepsilon}_R\bar{\mathbf{e}}$, represents the purely dielectric effect, the second $\hat{\Delta} : \mathbf{E^E}$ accounts for piezoelectric coupling, and the third $\hat{\chi}(\theta-\theta_1)$ accounts for pyroelectric coupling. Regarding the latter, temperature-induced polarization will occur when $\widehat{\chi}$ is non-zero and $\theta \neq \theta_1$ in (107). While $\bar{\varepsilon}_R$

is often referred to as the dielectric constant [39], its entries here in the context of geometric non-linearity are not fixed constants, but instead depend upon the elastic deformation. The materially linear framework of (102)–(108) is insufficient to address ferroelectric behavior, which requires a more detailed energy functional to account for transition temperatures and higher-order influences of polarization [20].

4.6. Diffusion of vacancies

Next consider diffusion of vacancies in the context of chemical potential (91), diffusion law (101), and free energy function (102). The chemical potential m in this case is

$$m = J^{E-1}(1 + \bar{A}\xi)^{-1}\bar{\upsilon}\xi + ez\hat{\phi} + J^E\alpha p, \tag{109}$$

leading to the flux equation

$$\bar{\zeta}^{\alpha} = -\bar{D}^{\alpha\beta}\{[J^{E-1}(1+\bar{A}\xi)^{-1}\bar{\upsilon}]\xi_{,\beta} + ez\hat{\phi}_{,\beta} + J^E\alpha p_{,\beta}$$
$$+ \xi[J^{E-1}(1+\bar{A}\xi)^{-1}\bar{\upsilon}]_{,\beta} + p[J^E\alpha]_{,\beta}\}. \tag{110}$$

The first term on the right of (110) causes vacancies to diffuse from regions of high concentration to regions of low concentration. The second term causes positively charged vacancies to diffuse from regions of high electrostatic potential to regions of low electrostatic potential, leading to a reduction in system energy since the vacancy charge density $ez\xi$ and electrostatic potential $\hat{\phi}$ are work conjugates in (66). The third term causes vacancies to diffuse from regions of high hydrostatic pressure to regions of low pressure $\alpha > 0$. The fourth and fifth terms reflect non-linear effects resulting from spatial gradients in property $\bar{\upsilon}$ (e.g. heterogeneous crystals), elastic volume changes, and vacancy concentration. Upon neglecting non-linear effects such that $1 + \bar{A}\xi \approx 1$ in a homogeneous body in the absence of elastic deformation, pressure gradients, and electric fields, (110) reduces to a version of Fick's Law

$$\bar{\zeta}^{\alpha} \approx -\bar{\upsilon}\bar{D}^{\alpha\beta}\xi_{,\beta}, \tag{111}$$

i.e. a familiar linear relationship between the flux of vacancies and the spatial gradient in vacancy concentration. The dependence of free energy upon vacancy density used in (102) is perhaps the simplest formulation that maintains elements of physical realism. The particular form used for the vacancy energy, or the parameter $\bar{\upsilon}$, can be estimated using arguments from chemical mixture theory [29] or free energy versus defect content results from lattice statics/dynamics calculations [11], at defect densities large enough such that interaction effects between neighboring defects become significant. More general functions than (102) are required to address all relevant couplings between defect content and bulk electromechanical and thermal responses. For example, the vacancy content in elastic dielectrics may alter the elastic moduli [14,21] and affect the piezoelectric coefficients. Furthermore, the vacancy energy and hence diffusion may be strongly affected by temperature, and could perhaps more realistically be a non-quadratic function of temperature and vacancy concentration in dielectric solids [14,15,63]. In the present treatment, no restrictions are placed on the diffusion coefficients $\bar{D}^{\alpha\beta}$, except that their matrix should be symmetric and positive semi-definite to ensure a positive rate of entropy production. It is well known that entries of $\bar{D}^{\alpha\beta}$ need not be constants, but instead may depend upon pressure and temperature [38]. Deviatoric stresses can affect the diffusion of point defects, as observed for creep mechanisms in polycrystals [33] and vacancy or interstitial migration in semiconductors [1]. Effects of stress directionality on diffusivity could be incorporated via specification of $\bar{D}^{\alpha\beta}$ dependent on the elastic strain.
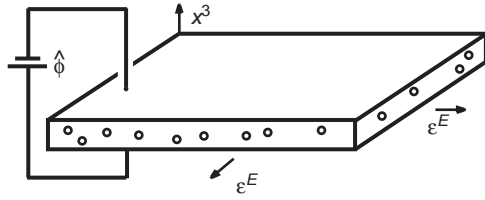
Fig. 3. Dielectric slab with vacancies subjected to biaxial lattice strain and applied electrostatic potential.

4.7. Example: diffusion under biaxial lattice strain

Consider the slab of material shown in Fig. 3, subjected to the uniform biaxial elastic strain field ε^E in the $x^1 - x^2$ plane, so that in Cartesian coordinates, $F_{.1}^{E1} = F_{.2}^{E2} = 1 + \varepsilon^E$ and $F_{.\alpha}^{Ea} = \delta_{.\alpha}^{a}$ otherwise. Potentials are applied to faces of the slab normal to x^3, with values of $\hat{\phi}$ differing on either face. Thus the voltages impose an electric field $-\nabla\hat{\phi}$, where ∇ is the spatial gradient operator in the x^3-direction. For example, when one face of the slab is grounded with $\hat{\phi} = 0$, the magnitude of the applied electric field is then the value of $\hat{\phi}$ at the opposite face divided by the thickness of the slab in the x^3-direction. For simplicity, the interfaces here are assumed to prevent global straining in the x^3-direction. The system corresponds physically to a dielectric film device [14–16,53]. In the physical system, the elastic strain ε^E may arise from a mismatch in lattice parameters across the interfaces, for example between the dielectric slab and neighboring substrates or electrodes, in conjunction with processing steps that may introduce residual thermal stresses [14,53]. Consider uniaxial diffusion with vacancy flux ζ parallel to the x^3-direction, in a dielectric solid with isotropic diffusivity d such that $\bar{D}^{\alpha\beta} = d\delta^{\alpha\beta}$. Under these conditions, flux equation (110) mapped to the spatial coordinate frame becomes

$$-\zeta/d = [(1 + \varepsilon^E)^{-2} - 2\alpha\xi]\upsilon\nabla\xi + [(1 + \varepsilon^E)^{-2}]ez\nabla\hat{\phi}, \qquad (112)$$

where $\upsilon = J^{E-1}\bar{\upsilon} = \rho\partial^2\psi/\partial\xi^2$. Terms in braces in (112) reduce to unity in the context of traditional, geometrically linear models in which finite deformations are not considered [18,37], wherein the chemical potential often exhibits the simple form $m = \upsilon\xi + ez\hat{\phi} + \alpha p$. In the scenario corresponding to Fig. 3, a spatially constant pressure p is assumed to complement the assumption of a constant elastic strain; hence possible effects of pressure gradients on diffusion are absent in (112).

Shown graphically in Fig. 4(a) is the normalized flux $-\zeta/(d\upsilon\nabla\xi)$ corresponding to the first term on the right of (112). Compressive strains $\varepsilon^E < 0$ and reductions in volume from vacancies $\alpha\xi < 0$ tend to increase the normalized flux, while tensile strains $\varepsilon^E > 0$ and positive volume changes $\alpha\xi > 0$ from vacancies tend to decrease the normalized flux. Interestingly, at very large concentrations $\alpha\xi \geqslant 0.2$ and tensile strains $\varepsilon^E \geqslant 0.6$, the instantaneous direction of flux would change since then $-\zeta/(d\upsilon\nabla\xi) < 0$, and vacancies would coalesce rather than migrate to areas of lower concentration. Shown in Fig. 4(b) is the normalized flux arising only from gradients in electrostatic potential, corresponding to the second term on the right of (112). Again, compressive strains $\varepsilon^E < 0$ tend to increase the flux while tensile strains $\varepsilon^E > 0$ tend to decrease the flux. In summary, large elastic deformations $|\varepsilon^E| \geqslant 0.1$ and large vacancy concentrations $|\alpha\xi| \geqslant 0.1$ are predicted according to (112) and Fig. 4 to influence vacancy migration. However, stress and vacancy content may also affect the diffusivity d [38]; such effects would depend on the particular dielectric material comprising the slab and are not considered in Fig. 4, wherein d is assumed constant. Furthermore, dislocation nucleation or fracture could ensue in dielectric solids to relieve
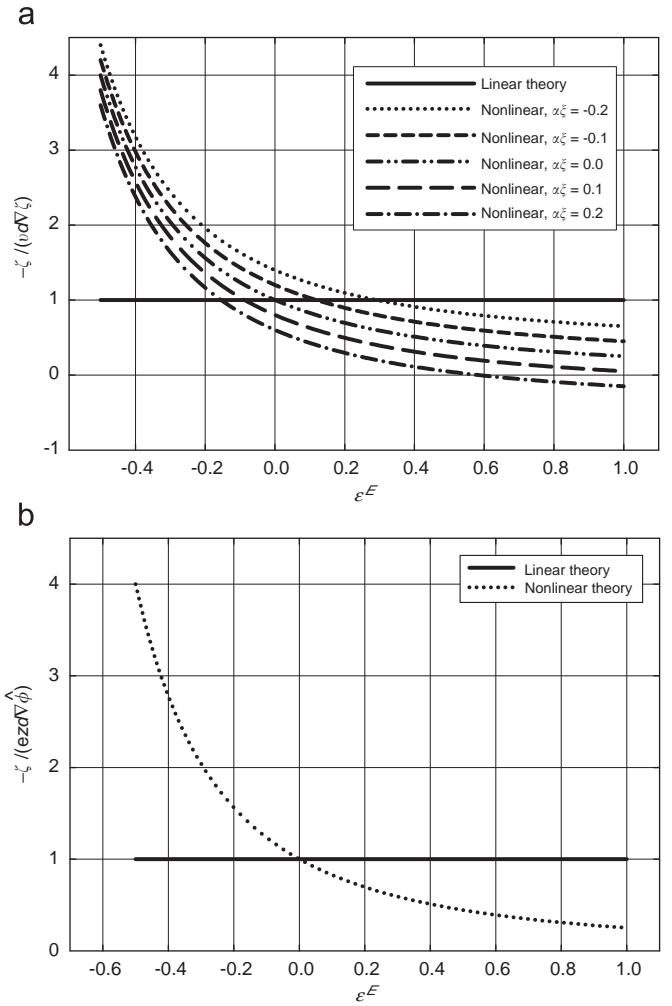

Fig. 4. Normalized vacancy flux driven by (a) concentration gradient and (b) electrostatic potential gradient.

potentially large elastic strains; such effects are also not considered here.

5. Conclusions

A model framework has been formulated for the electromechanical behavior of dielectric crystalline solids subjected to large deformations. These deformations consist of thermoelastically recoverable stretch and rigid body rotation, as well as volumetric changes resulting from voids or vacancies. Charge transport resulting from diffusion is considered; the motion of electronic charges occurring at faster time scale (i.e., electric currents) is not. A model for elastic dielectrics without defects, in the quasi-electrostatic approximation, has been presented first, to lend context to the more general theory allowing for vacancies developed later. The latter theory may be the first to consider finite volume changes resulting from charged vacancies in ionic crystals in the context of multiplicative inelasticity. Governing equations, constitutive relations, and kinetic equations are cast in the relaxed intermediate configuration implied by the multiplicative decomposition. Non-linear electromechanical effects associated with Maxwell's stress are retained. Effects of spatial gradients of vacancy concentration, electrostatic potential, and hydrostatic pressure arise naturally in the thermodynamically admissible diffusion equation for the vacancy flux, without assumption of such kinetic law dependencies a priori. Upon assumption of a quadratic free energy

dependence on vacancy density, Fick-type diffusion is recovered in the linearized limit, in the absence of electrostatic and pressure effects. However, in the non-linear regime, large elastic deformations and large vacancy concentrations may influence the vacancy flux.

Appendix A. List of symbols

$\mathbf{X}, X^A$	reference coordinates
$\mathbf{x}, x^a$	spatial coordinates
φ	motion
t	time
B_0	reference configuration
B	current configuration
$\bar{B}$	intermediate configuration
$\mathbf{G}_A$	reference basis vectors
$\mathbf{g}_a$	spatial basis vectors
$\mathbf{G}, G_{AB}$	reference metric tensor
$\mathbf{g}, g_{ab}$	spatial metric tensor
$\bar{\mathbf{g}}, \bar{g}_{\alpha\beta}$	intermediate metric tensor
$\mathbf{1}, \delta^A_{.B}, \delta^a_{.b}, \delta^\alpha_{.\beta}$	unit tensor
$\bar{\boldsymbol{\delta}}, \bar{\delta}^\alpha_{.A}$	shifter
$\overset{G}{\Gamma}{}^{.A}_{BC}$	reference Christoffel symbols
$\overset{g}{\Gamma}{}^{.a}_{bc}$	spatial Christoffel symbols
$\overset{G}{\nabla}_A$	reference covariant derivative
$\overset{g}{\nabla}_a$	spatial covariantderivative
$\bar{\nabla}_\alpha$	intermediate covariant derivative
$\boldsymbol{\varepsilon}, \varepsilon^{abc}$	permutation tensor
ρ_0	reference mass density
ρ	spatial mass density
$\bar{\rho}$	intermediate mass density
$\mathbf{F}, F^a_{.A}$	deformation gradient
$\mathbf{F^E}, F^{Ea}_{.\alpha}$	elastic deformation gradient
$\mathbf{F^V}, F^{V\alpha}_{.A}$	vacancy deformation gradient
J	Jacobian determinant of $\mathbf{F}$
J^E	Jacobian determinant of $\mathbf{F^E}$
J^V	Jacobian determinant of $\mathbf{F^V}$
$\mathbf{C}, C_{AB}$	right Cauchy–Green deformation
$\mathbf{C^E}, C^E_{\alpha\beta}$	elastic deformation
$\mathbf{E}, E_{AB}$	Lagrangian strain
$\mathbf{E^E}, E^E_{\alpha\beta}$	elastic strain
ε^E	elastic stretch
$\mathbf{v}, v^a$	spatial velocity
$\mathbf{L}, L^a_{.b}$	spatial velocity gradient
$\mathbf{L^V}, L^{V\alpha}_{.\beta}$	vacancy velocity gradient
$\mathbf{D}, D_{ab}$	spatial deformation rate
$\mathbf{W}, W_{ab}$	spin
dV	reference volume element
dv	spatial volume element
$d\bar{V}$	intermediate volume element
$\mathbf{N}\,dS$	reference surface element
$\mathbf{n}\,ds$	spatial surface element
$\hat{\mathbf{E}}, \hat{E}^A$	reference electric field
$\hat{\mathbf{e}}, \hat{e}^a$	spatial electric field
$\bar{\mathbf{e}}, \bar{e}^\alpha$	intermediate electric field
$\hat{\Phi}$	reference electrostatic potential
$\hat{\phi}$	spatial electrostatic potential
$\hat{\mathbf{f}}, \hat{f}^a$	Lorentz force
q	point charge
$q^{(i)}$	electric charge of carrier i

$z^{(i)}$	valence of carrier i
$\hat{n}^{(i)}$	no. of carriers per spatial volume
e	charge magnitude of an electron
ε_0	permittivity of vacuum
$\hat{\sigma}$	free surface charge density
$\hat{\omega}$	internal surface charge density
$\hat{\rho}_0$	reference free charge density
$\hat{\rho}$	spatial free charge density
$\hat{\rho}^V$	charge density of vacancies
$\hat{\rho}^C$	charge density of electrons/holes
$\hat{\mathbf{P}}, \hat{P}^A$	reference polarization
$\hat{\mathbf{p}}, \hat{p}^a$	spatial polarization
$\bar{\mathbf{p}}, \bar{p}^\alpha$	intermediate polarization
$\hat{\mathbf{D}}, \hat{D}^A$	reference electric displacement
$\hat{\mathbf{d}}, \hat{d}^a$	spatial electric displacement
$\bar{\mathbf{d}}, \bar{d}^\alpha$	intermediate electric displacement
$\bar{\mathbf{b}}, \bar{b}^a$	mechanical body force
$\hat{\mathbf{b}}, \hat{b}^a$	electromechanical body force
$\mathbf{t}, t^a$	mechanical traction
$\mathbf{T}, T^a$	total traction
$\boldsymbol{\sigma}, \sigma^{ab}$	Cauchy stress
$\hat{\boldsymbol{\tau}}, \hat{\tau}^{ab}$	Maxwell stress
$\boldsymbol{\tau}, \tau^{ab}$	total stress
$\mathbf{P}, P^{aA}$	first Piola–Kirchhoff (P–K) stress
$\bar{\mathbf{P}}, \bar{P}^{a\alpha}$	elastic first P–K stress
$\boldsymbol{\Sigma}, \Sigma^{AB}$	second P–K stress
$\bar{\boldsymbol{\Sigma}}, \bar{\Sigma}^{\alpha\beta}$	elastic second P–K stress
p	Cauchy pressure
$\mathscr{K}$	kinetic energy
$\mathscr{E}$	total internal (system) energy
$\mathscr{D}$	thermochemical energy
$\mathscr{P}$	total external power
Ω	electrostatic power per unit volume
θ	absolute temperature
ψ	free energy per unit mass
e	internal energy per unit mass
η	entropy per unit mass
r	heat source per unit mass
c	specific heat per unit mass
Y	thermal energy
ϕ_0	reference vacancy volume fraction
$\bar{\phi}$	intermediate vacancy fraction
ξ_0	no. vacancies per reference volume
ξ	no. vacancies per spatial volume
α	net volume per vacancy
$\bar{A}$	normalized volume per vacancy
m	chemical potential
$\boldsymbol{\zeta}_0, \zeta^A_0$	reference vacancy flux
$\boldsymbol{\zeta}, \zeta^a$	spatial vacancy flux
$\bar{\boldsymbol{\zeta}}, \bar{\zeta}^\alpha$	intermediate vacancy flux
$\bar{\mathbf{D}}, \bar{D}^{\alpha\beta}$	intermediate vacancy diffusivity
d	isotropic diffusivity
$\mathbf{Q}, Q^A$	reference heat flux
$\mathbf{q}, q^a$	spatial heat flux
$\bar{\mathbf{q}}, \bar{q}^\alpha$	intermediate heat flux
$\mathbf{K}, K^{AB}$	reference thermal conductivity
$\bar{\mathbf{K}}, \bar{K}^{\alpha\beta}$	intermediate thermal conductivity
$\boldsymbol{\beta}, \beta^{ab}$	spatial thermal stress coefficients
$\bar{\boldsymbol{\beta}}, \bar{\beta}^{\alpha\beta}$	intermediate thermal stress coefficients
$\boldsymbol{\chi}, \chi^a$	spatial pyroelectric coefficients
$\bar{\boldsymbol{\chi}}, \bar{\chi}^\alpha$	intermediate pyroelectric coefficients
$\mathbb{C}, \mathbb{C}^{ABCD}$	reference elastic coefficients

$\bar{\mathbb{C}}, \bar{\mathbb{C}}^{\alpha\beta\chi\delta}$	intermediate elastic coefficients
$\boldsymbol{\Lambda}, \Lambda^{AB}$	reference dielectric susceptibility
$\boldsymbol{\Lambda}, \bar{\Lambda}^{\alpha\beta}$	intermediate susceptibility
$\boldsymbol{\Delta}, \Delta^{ABC}$	reference piezoelectric coefficients
$\bar{\boldsymbol{\Delta}}, \bar{\Delta}^{\alpha\beta\chi}$	intermediate piezoelectric coefficients
$\bar{\boldsymbol{\varepsilon}}_{\mathbf{R}}, \bar{\varepsilon}_R^{\alpha\beta}$	relative dielectric permittivity
υ	spatial vacancy energy coefficient
$\bar{\upsilon}$	intermediate vacancy energy coefficient
$\bar{c}$	intermediatespecific heat coefficient
θ_0, θ_1	reference temperatures

References

[1] M.J. Aziz, Thermodynamics of diffusion under pressure and stress: relation to point defect mechanisms, Appl. Phys. Lett. 70 (2005) 2810–2812.

[2] D.J. Bammann, E.C. Aifantis, A damage model for ductile metals, Nucl. Eng. Des. 116 (1989) 355–362.

[3] N. Bernstein, H.J. Gostis, D.A. Papaconstantopoulos, M.J. Mehl, Tight-binding calculations of the band structure and total energies of the various polytypes of silicon carbide, Phys. Rev. B 71 (2005) 075203.

[4] B.A. Bilby, L.R.T. Gardner, A.N. Stroh, Continuous distributions of dislocations and the theory of plasticity, in: Proceedings of the Ninth International Congress on Applied Mechanics, Bruxelles, vol. 8, 1957, pp. 35–44.

[5] H.E. Bommel, W.P. Mason, A.W. Warner, Dislocations, relaxations, and anelasticity of crystal quartz, Phys. Rev. 102 (1956) 64–71.

[6] M. Born, K. Huang, Dynamical Theory of Crystal Lattices, Clarendon, Oxford, 1954.

[7] R.M. Bowen, Toward a thermodynamics and mechanics of mixtures, Arch. Ration. Mech. Anal. 24 (1967) 370–403.

[8] J.C. Brice, Crystals for quartz resonators, Rev. Mod. Phys. 57 (1985) 105–147.

[9] R. Chang, Creep of Al_2O_3 single crystals, J. Appl. Phys. 31 (1960) 484–487.

[10] K.L. Chowdhury, M. Epstein, P.G. Glockner, On the thermodynamics of non-linear elastic dielectrics, Int. J. Non-Linear Mech. 13 (1978) 311–322.

[11] J.D. Clayton, P.W. Chung, An atomistic-to-continuum framework for nonlinear crystal mechanics based on asymptotic homogenization, J. Mech. Phys. Solids 54 (2006) 1604–1639.

[12] J.D. Clayton, D.J. Bammann, D.L. McDowell, Anholonomic configuration spaces and metric tensors in finite elastoplasticity, Int. J. Non-Linear Mech. 39 (2004) 1039–1049.

[13] J.D. Clayton, D.J. Bammann, D.L. McDowell, A geometric framework for the kinematics of crystals with defects, Philos. Mag. 85 (2005) 3983–4010.

[14] J.D. Clayton, P.W. Chung, M.A. Grinfeld, W.D. Nothwang, Kinematics, electromechanics, and kinetics of dielectric and piezoelectric crystals with lattice defects, Int. J. Eng. Sci. 46 (2008) 10–30.

[15] J.D. Clayton, P.W. Chung, M.A. Grinfeld, W.D. Nothwang, Continuum modeling of charged vacancy migration in elastic dielectric solids, with application to perovskite thin films, Mech. Res. Commun. 35 (2008) 57–64.

[16] M.W. Cole, W.D. Nothwang, C. Hubbard, E. Ngo, M. Ervin, Low dielectric loss and enhanced tunability of $Ba_{0.6}Sr_{0.4}TiO_3$ based thin films via material compositional design and optimized film processing methods, J. Appl. Phys. 93 (2003) 9218–9225.

[17] B.D. Coleman, W. Noll, The thermodynamics of elastic materials with heat conduction and viscosity, Arch. Ration. Mech. Anal. 13 (1963) 167–178.

[18] H. Conrad, Space charge and the dependence of the flow stress of ceramics on an applied electric field, Scr. Mater. 44 (2001) 311–316.

[19] D. Damjanovic, Ferroelectric, dielectric and piezoelectric properties of ferroelectric thin films and ceramics, Rep. Prog. Phys. 61 (1998) 1267–1324.

[20] A.F. Devonshire, Theory of ferroelectrics, Philos. Mag. 3 (1954) 85–130.

[21] G.J. Dienes, A theoretical estimate of the effect of radiation on the elastic constants of simple metals, Phys. Rev. 86 (1952) 228–234.

[22] A. Dorfmann, R.W. Ogden, Nonlinear electroelasticity, Acta Mech. 174 (2005) 167–183.

[23] T.C. Doyle, J.L. Ericksen, Nonlinear elasticity, in: H.L. Dryden, T. Von Karman (Eds.), Advances in Applied Mechanics, vol. IV, Academic Press, New York, 1956, pp. 53–115.

[24] C. Eckart, The thermodynamics of irreversible processes I. The simple fluid, Phys. Rev. 58 (1940) 267–269.

[25] C. Eckart, The thermodynamics of irreversible processes IV. The theory of elasticity and anelasticity, Phys. Rev. 73 (1948) 373–382.

[26] J.L. Ericksen, The Cauchy and Born hypothesis for crystals, in: M.E. Gurtin (Ed.), Phase Transformations and Material Instabilities in Solids, 1984, pp. 61–78.

[27] A.C. Eringen, On the foundations of electroelastostatics, Int. J. Eng. Sci. 1 (1963) 127–153.

[28] J.D. Eshelby, The continuum theory of lattice defects, in: F. Seitz, D. Turnbull (Eds.), Solid State Physics, 3, Academic Press, New York, 1956, pp. 79–144.

[29] V. Fried, H.F. Hameka, U. Blukis, Physical Chemistry, Macmillan, New York, 1977.

[30] E.P. Hadjigeorgiou, V.K. Kalpakides, C.V. Massalas, A general theory for elastic dielectrics—part I. The vectorial approach, Int. J. Non-Linear Mech. 34 (1999) 831–841.

[31] M.A. Grinfeld, Thermodynamic Methods in the Theory of Heterogeneous Systems, Wiley, New York, 1991.

[32] M.A. Grinfeld, P.M. Hazzledine, Role of vacancies in slow evolution of a traction-free interface, Europhys. Lett. 37 (1997) 409–413.

[33] C. Herring, Diffusional viscosity of a polycrystalline solid, J. Appl. Phys. 21 (1950) 437–445.

[34] J.P. Hirth, J. Lothe, Theory of Dislocations, Wiley, New York, 1982.

[35] M.F. Horstemeyer, J. Lathrop, A.M. Gokhale, M. Dighe, Modeling stress state dependent damage evolution in a cast Al–Si–Mg aluminum alloy, Theor. Appl. Fract. Mech. 33 (2000) 31–47.

[36] C.S. Hwang, B.T. Lee, C.S. Kang, K.H. Lee, H.J. Cho, H. Hideki, W.D. Kim, S.I. Lee, M.Y. Lee, Depletion layer thickness and Schottky type carrier injection at the interface between Pt electrodes and (Ba, Sr)TiO$_3$ thin films, J. Appl. Phys. 85 (1999) 287–295.

[37] J. Jamnik, R. Raj, Space-charge-controlled diffusional creep: volume diffusion case, J. Am. Ceram. Soc. 79 (1996) 193–198.

[38] R.N. Jeffery, D. Lazarus, Calculating activation volumes and activation energies from diffusion measurements, J. Appl. Phys. 41 (1970) 3186–3187.

[39] K.M. Johnson, Variation of dielectric constant with voltage in ferroelectrics and its application to parametric devices, J. Appl. Phys. 33 (1962) 2826–2831.

[40] K.L. Kliewer, J.S. Koehler, Space charge in ionic crystals. I. General approach with application to NaCl, Phys. Rev. 140 (1965) 1226–1240.

[41] M.L. Kronberg, Plastic deformation of single crystals of sapphire: basal slip and twinning, Acta Metall. 5 (1957) 507–524.

[42] E. Kroner, The differentiable geometry of elementary point and line defects in Bravais crystals, Int. J. Theor. Phys. 29 (1990) 1219–1237.

[43] L.D. Landau, E.M. Lifshitz, Electrodynamics of Continuous Media, Pergamon Press, Oxford, 1960.

[44] E.H. Lee, Elastic–plastic deformation at finite strains, ASME J. Appl. Mech. 36 (1969) 1–6.

[45] L.E. Malvern, Introduction to the Mechanics of a Continuous Medium, Prentice-Hall, NJ, 1969.

[46] A. Many, G. Rakavy, Theory of transient space-charge-limited currents in solids in the presence of trapping, Phys. Rev. 126 (1962) 1980–1988.

[47] J.E. Marsden, T.J.R. Hughes, Mathematical Foundations of Elasticity, Dover, New York, 1983.

[48] G.A. Maugin, On the covariant equations of the relativistic electrodynamics of continua. III. Elastic solids, J. Math. Phys. 19 (1978) 1212–1219.

[49] G.A. Maugin, Continuum Mechanics of Electromagnetic Solids, North-Holland, Amsterdam, 1988.

[50] R.M. McMeeking, C.M. Landis, S.M.A. Jimenez, A principle of virtual work for combined electrostatic and mechanical loading of materials, Int. J. Non-Linear Mech. 42 (2007) 831–838.

[51] A.P. Migorodsky, M.B. Smirnov, E. Abdelmounim, T. Merle, P.E. Quintard, Molecular approach to the modeling of elasticity and piezoelectricity of SiC polytypes, Phys. Rev. B 52 (1995) 3993–4000.

[52] R.D. Mindlin, Elasticity, piezoelectricity, and crystal lattice dynamics, J. Elasticity 2 (1972) 217–282.

[53] W.D. Nothwang, M.W. Cole, S.G. Hirsch, Grain growth and residual stress in BST thin films, Integ. Ferroelect. 71 (2005) 107–113.

[54] E. Pan, Mindlin's problem for an anisotropic piezoelectric half-space with general boundary conditions, Proc. R. Soc. London A 458 (2001) 181–208.

[55] S. Saha, S.B. Krupanidhi, Microstructure related influence on the electrical properties of pulsed laser ablated (Ba, Sr)TiO$_3$ thin films, J. Appl. Phys. 88 (2000) 3506–3513.

[56] J.S. Speck, W. Pompe, Domain configurations due to multiple misfit relaxation mechanisms in epitaxial thin films. I. Theory, J. Appl. Phys. 76 (1994) 466–476.

[57] J.A. Stratton, Electromagnetic Theory, McGraw-Hill, New York, 1941.

[58] H.F. Tiersten, On the nonlinear equations of thermoelectroelasticity, Int. J. Eng. Sci. 9 (1971) 587–604.

[59] R.A. Toupin, The elastic dielectric, J. Ration. Mech. Anal. 5 (1956) 849–915.

[60] D.K. Vu, P. Steinmann, Nonlinear electro- and magneto-elastostatics: material and spatial settings, Int. J. Solids Struct. 44 (2007) 7891–7905.

[61] J. Weertman, Theory of steady-state creep based on dislocation climb, J. Appl. Phys. 26 (1955) 1213–1217.

[62] Y. Xiao, The influence of oxygen vacancies on domain patterns in ferroelectric perovskites, Ph.D. Thesis, California Institute of Technology, Pasadena, CA, 2004.

[63] Y. Xiao, V.B. Shenoy, K. Bhattacharya, Depletion layers and domain walls in semiconducting ferroelectric thin films, Phys. Rev. Lett. 95 (2005) 247603.

[64] W. Zhang, K. Bhattacharya, A computational model of ferroelectric domains. Part I: model formulation and domain switching, Acta Mater. 53 (2005) 185–198.

NO. OF
COPIES ORGANIZATION

  1   DEFENSE TECHNICAL
 (PDF   INFORMATION CTR
 only)   DTIC OCA
         8725 JOHN J KINGMAN RD
         STE 0944
         FORT BELVOIR VA 22060-6218

  1   DIRECTOR
         US ARMY RESEARCH LAB
         IMNE ALC HRR
         2800 POWDER MILL RD
         ADELPHI MD 20783-1197

  1   DIRECTOR
         US ARMY RESEARCH LAB
         RDRL CIM L
         2800 POWDER MILL RD
         ADELPHI MD 20783-1197

  1   DIRECTOR
         US ARMY RESEARCH LAB
         RDRL CIM P
         2800 POWDER MILL RD
         ADELPHI MD 20783-1197

         ABERDEEN PROVING GROUND

  1   DIR USARL
         RDRL CIM G (BLDG 4600)